Semi-solid extrusion 3D printing in drug delivery and biomedicine: Personalised solutions for healthcare challenges

Iria Seoane-Viaño, Patricija Januskaite, Carmen Alvarez-Lorenzo, Abdul W. Basit, Alvaro Goyanes

PII: S0168-3659(21)00100-0

DOI: https://doi.org/10.1016/j.jconrel.2021.02.027

Reference: COREL 10820

To appear in: *Journal of Controlled Release*

Received date: 24 December 2020

Revised date: 19 February 2021

Accepted date: 22 February 2021

Please cite this article as: I. Seoane-Viaño, P. Januskaite, C. Alvarez-Lorenzo, et al., Semi-solid extrusion 3D printing in drug delivery and biomedicine: Personalised solutions for healthcare challenges, *Journal of Controlled Release* (2021), https://doi.org/10.1016/j.jconrel.2021.02.027

Semi-solid extrusion 3D printing in drug delivery and biomedicine: personalised solutions for healthcare challenges

Iria Seoane-Viaño[1], Patricija Januskaite[2], Carmen Alvarez-Lorenzo[3], Abdul W. Basit[2,4*], Alvaro Goyanes[2,3,4*]

[*]Correspondence: Alvaro Goyanes (a.goyanes@fabrx.co.uk) and Abdul W. Basit (a.basit@ucl.ac.uk)

[1]Department of Pharmacology, Pharmacy and Pharmaceutical Technology, Paraquasil Group, Faculty of Pharmacy, University of Santiago de Compostela (USC), and Health Research Institute of Santiago de Compostela (IDIS), Santiago de Compostela, 15782, Spain.

[2]Department of Pharmaceutics, UCL School of Pharmacy, University College London, 29-39 Brunswick Square, London WC1N 1AX, UK.

[3]Departamento de Farmacología, Farmacia y Tecnología Farmacéutica, I+D Farma Group (GI-1645), Universidade de Santiago de Compostela, 15782, Spain.

[4]FabRx Ltd., 3 Romney Road, Ashford, Kent, TN24 0RW, UK.

ABSTRACT

Three-dimensional (3D) printing is an innovative additive manufacturing technology, capable of fabricating unique objects in a layer-by-layer manner. Semi-solid extrusion (SSE) is a subset of material extrusion 3D printing, based on the sequential deposition of layers of gel or paste to create an object of a desired size and shape. In comparison to other extrusion-based technologies, SSE 3D printing employs low printing temperatures making it suitable for drug delivery and biomedical applications, and the use of disposable syringes provides benefits in meeting critical quality requirements for pharmaceutical use. Besides pharmaceutical manufacture, SSE 3D printing has attracted increasing attention in the field of bioelectronics, particularly in the manufacture of biosensors capable of measuring physiological parameters or as a means to trigger drug release from medical devices. This review begins by highlighting the major printing process parameters and material properties that influence the feasibility of transforming a 3D design into a 3D object, followed by a discussion of the current SSE 3D printing developments and applications in the fields of pharmaceutics, bioprinting and bioelectronics. Finally, the advantages and limitations offered by this technology are

explored, focusing on its potential clinical applications and suitability for preparing personalised medicines.

Keywords: 3D printing; Micro-extrusion; Direct Ink Writing; Personalized pharmaceuticals and medicines; 3D printed drug products; Rheology and food printing.

1. Introduction

Three-dimensional printing (3DP) is an additive manufacturing method that enables the construction of bespoke objects in a layer-by-layer manner (1-3). The term 3DP encompasses an array of different technologies, which can be classified based on the American Society for Testing and Materials (ASTM) standards into seven main categories: binder jetting, directed energy deposition, material extrusion, material jetting, powder bed fusion, sheet lamination, and vat photopolymerization (4). However in the pharmaceutical field, only a few technologies and subcategories are currently used: binder jetting (5-8), material extrusion (fused deposition modelling (FDM) (9-12), material jetting (13-16), direct powder extrusion (DPE) (17-19) and semi-solid extrusion (SSE) (20-24)), selective laser sintering (SLS) (25-29) (a subcategory of powder bed fusion technology) and vat photopolymerization (30-33) (which includes technologies like stereolithography (SLA), digital light processing (DLP) and continuous liquid interface production (CLIP)). Independent of the technique used, the first step involves the use of a computer aided design (CAD) software to design the object to be printed. Next, the 3D model is divided into a series of layers and exported to the 3D printer as an .stl file to be fabricated in a layer-by-layer fashion. As a result, an individualised object of the desired shape and size can be created (34-37).

Semi-solid extrusion (SSE) is a material extrusion technique based on the deposition of a gel or paste in sequential layers to create the 3D object. Upon extrusion, the material hardens, allowing the subsequent tiers to be supported by the ones underneath (38). The key differences between SSE and the other material extrusion techniques like FDM or DPE are in the feedstock materials used (39). In SSE, the starting material is a semi-solid or semi-molten material, whereas in FDM and DPE the printing material is in the form of a solid filament or powder, respectively (17, 40-42). In the literature, SSE is

also known as pressure-assisted microsyringe (PAM) printing (43-45), robocasting or robotic material extrusion (46), cold extrusion-based printing (47), hydrogel-forming extrusion (48), melting extrusion (48), thermal extrusion (49), soft-material extrusion (48), melting solidification printing process (50), direct ink writing (51), hot-melt ram extrusion (52), hot-melt pneumatic extrusion (53) and micro-extrusion (54).

The physical nature of the feedstock material is what makes SSE especially relevant for bioprinting applications (55). The low temperatures needed for printing allows the creation of living cell structures, such as aortic valves (56), or the repair of damaged tissues (57). Additionally, the use of disposable syringes and pre-filled cartridges contributes to this technology meeting the critical quality requirements demanded by regulatory agencies.

The unique attributes of this technology are now being explored in drug development to produce novel dosage forms (58). Printlets™ (3D printed tablets) and other devices can be produced in a matter of minutes in a single-step process, making SSE a perfect candidate for its inclusion in clinical settings or research laboratories. SSE 3DP was used for the first clinical study that prepared on-demand, personalized printlets in a hospital setting (59), where chewable dosage forms in different flavours and colour profiles were prepared on site at a pharmacy hospital and administered to children with a rare metabolic disease. Chewable printlets have shown to be one of the preferred types of formulations by children when compared to printlets prepared using different 3DP technologies (DLP, SLS, FDM and SSE) (60). The study evaluated children's visual preferences for the different 3D printed formulations. Although the DLP and SLS printlets were the most visually appealing, when the children were informed that the SSE printlet was chewable, most changed their preferences and selected the chewable dosage form as their favourite.

Nevertheless, the applications of SSE do not end in drug development. This technique is also widely used in food printing (61) and is beginning to gain interest in the printing of electronic devices (62). The increasing amount of research using SSE and the positive results obtained from the work highlighted set a promising precedent for its future implementation in healthcare (63). The following section will describe and discuss the

SSE 3DP process and crucial parameters that influence the printability and quality of the final 3D object,

2. Semi-solid extrusion printing process

Similar to other 3DP technologies, the SSE printing process begins with the generation of the desired 3D model structure using a computer aided design (CAD) software, which is then converted to an .stl file and subsequently loaded to the printer equipment. If any changes in the final object are required, it can be achieved by simply modifying the starting CAD file (64). Since the entire process is a computer-controlled procedure, production time and cost, as well as manual labour are reduced, a major advantage of 3DP in comparison with conventional manufacturing processes (34).

2.1. Extrusion

The most characteristic feature of SSE is the extrusion process. The feedstock material is in the form of a solid that possesses a relatively low melting point, or in a semisolid state, such as in the form of a gel or paste which is contained within a syringe (38). To acquire the right gel consistency, the printing materials can be heated or mixed with a solvent or mixture of solvents. The extrusion of the material through the syringe can be carried out by means of a pneumatic, mechanical or solenoid-based system (Figure 1) (65).

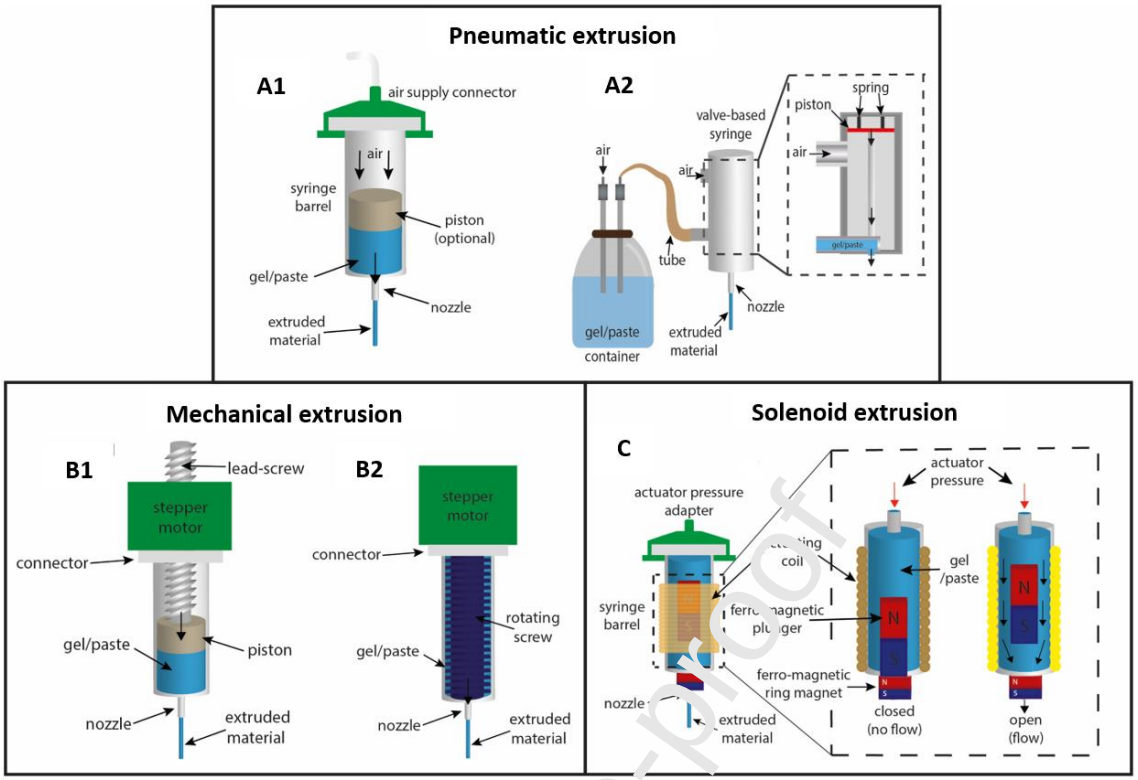

Figure 1. SSE 3DP extrusion mechanisms: (A) pneumatic extrusion including (A1) valve-free and (A2) valve-based, (B) mechanical extrusion including (B1) piston- or (B2) screw-driven and (C) solenoid extrusion.

2.1.1. Pneumatic-based systems

Pneumatic-based extrusion systems utilize pressurized air to compress and extrude the material (55). The air pressure supply is directly connected to the syringe barrel, the nozzle of which may have a valve to control the air channel in the printhead via on-off valve switching, closing the channel when the valve is off (Figure 1). This valve-based mechanism is generally used to prevent material release when no pressure is applied, and is highly recommended for low-viscosity materials, such as bioinks (55). On the other hand, the valve-free system is widely preferred due to its simplicity, and the materials commonly used in pharmaceutical SSE printing, such as hydrogels, present an adequate viscosity for use with this configuration (66). Pneumatically driven systems generally have a high degree of precision and their response time after starting the extrusion process is rapid, as the syringe barrel can be instantly pressurized. Additionally, the gas can reach significant pressures without compromising the integrity of the system, making this extrusion process suitable for printing highly viscous materials (55).

2.1.2. Mechanical-based system

Mechanical-based extrusion systems apply a mechanical force directly to the syringe (55), and can be designed in piston- or screw-driven configurations (Figure 1). The piston-based system provides greater control over the extrusion flow, while the screw-based system provides more spatial control and is capable of dispensing materials with higher viscosities than the piston-based system (54). The mechanism is simpler than the pneumatic system, and is also more affordable and easier to transport, lacking the need for an air compressor apparatus (55). In addition, this system allows the easy exchange of syringes that can be replaced in a quick manner, resulting in a faster printing process.

2.1.3. Solenoid extrusion printing

Solenoid extrusion utilises electrical pulses to open a valve located at the base of the syringe (55). The pulse terminates the magnetic pull force generated between a floating ferromagnetic plunger and a ferromagnetic ring magnet, which allows the dispensing of sub-μL volumes of material (Figure 1). This system is advantageous for the extrusion of low viscosity bioink solutions with ionic or ultraviolet (UV) irradiation-based crosslinking mechanisms, and is not suitable for printing the viscous materials used in pharmaceuticals (55). Moreover, there are a number of factors affecting the reproducibility of this extrusion system, such as the time lapse between the energization of the coil and the valve opening, which may result in an uneven deposition of material (65).

2.2. Printing process

During the printing process, the gel or paste is extruded through a nozzle at the base of the syringe (38). The nozzle diameter is a parameter that affects the printing precision considerably (67). The common rule is to select the smallest nozzle tip that allows for easy material extrusion, and to build an object with high resolution and smooth surface. Larger nozzle diameters extrude consistent strands but the final object resolution and printing accuracy is lower, whereas the smaller nozzle diameters are convenient for producing higher resolution objects (68). On the other hand, the risk of collapse is lower if a large nozzle is used, since the number of individual strands and therefore the number of contact points is lower, making the structure more rigid. Another potential reason for greater structure stability may be that the risk of blockage is higher for

smaller nozzle diameters, causing heterogeneities that may reduce the stability of the object (69). It is important to notice that the required printing time increases greatly when using a small nozzle size.

The nozzle travel speed and extrusion rate are also important factors in extrusion-based 3DP (67). In general, a high nozzle travel speed results in less material deposition, producing strands with smaller diameters which could also induce extruded strand breakage. Conversely, a slow travel speed may result in flow instabilities and the formation of imperfections. Regarding extrusion rate, high extrusion rates produce larger extruded filament diameters as a result of greater material volume extrusion, whilst low extrusion rates lead to an inconsistent material deposition (70).

In printing processes that depend on the heating of the feedstock material, the printing temperature is another parameter that should be fine-tuned as the viscosity of the material to be printed is in direct correlation with the temperature (20). Prior to printing, the syringe mixture is heated until it reaches a viscosity low enough to be extruded through the tip nozzle. However, if the material is too extensively liquefied, the structure will be incapable of retaining its shape (71). A printing temperature that is too high may also result in over-extrusion, whereby material flows in an uncontrollable manner. On the other hand, if it is too viscous, the nozzle may clog and the material would not flow, which could also damage the extrusion mechanism. Not only the heating of the syringe, but also the composition of the feedstock material can be modified to obtain a more viscous or liquefied formulation (65).

The positioning of the extrusion head when printing is also a critical factor in achieving successful extrusion printing (67). The distance between the nozzle and the build plate (or printing platform) must be calibrated according to the viscosity of the material. If the distance is too large, the extruded material may accumulate at the tip of the nozzle and not adhere to the printing platform properly; whilst if it is too close, there could be an insufficient and inconsistent material flow, resulting in incomplete deposition. After calibration, some printers are pre-programmed to print an arbitrary shape to ensure a continuous flow of material (38). The position of the printer head is orientated using a computer-controlled motor system and can move up-down and left-right to cover the Z, X and Y axes.

After the material extrusion, the effect of gravity may cause the material to change shape over time, and the object size may vary depending on the cooling or drying process (72). Moreover, the initial extruded layer should display good adhesion to the build plate, but not too much so that the printed object can be easily removed once the process is complete. Build plates can be made of different material, being glass commonly used, however, it is not the best surface for most of the extruded materials. Specialised tape (e.g. painter's tape, Kapton tape) are often employed to improve the adhesion of the material to the printing bed (20). In addition, the distance from the nozzle to the build plate should be kept to a minimum to prevent cooling of the extrudate before coming into contact with the build plate (73). A common problem arising during the printing process is material warping or 'curling', which is the twisting of layer outer edges as a result of exposure to heat or moisture (74). It is most evident in the first printed layer and is caused by uneven cooling of the extrudate. Depending on the characteristics of the material, some bed plates can be heated or cooled. A heated build plate can minimize material warping by limiting stress on the base layers, while a cooled build plate can aid in the solidification process of less viscous materials (71). In either case, the temperature requires adequate control to ensure the best performance of the printing process.

2.3. Solidification process

The use of heat or solvents will define the cooling or drying post-printing process, although there are other less known strategies to achieve solidification (75):

i) If the material is extruded using heat, this can be done immediately prior to extrusion and the solidification process will be determined by the cooling of the material. The printing temperature must be optimized to achieve an adequate material viscosity. Excessive heating can liquefy the material too much and make it difficult to rapidly cool it down to allow successive layers to print on top, and insufficient heating could cause the material to solidify at the tip of the syringe nozzle and cause blockage (71).

ii) In the event that a solvent or combination of solvents are used, a final step of solvent evaporation will be required to ensure solidification via solvent removal by placing the dosage forms in, for example, a vacuum oven.

iii) Other strategies to achieve solidification of the object include the use of inks composed of monomers/oligomers and photoinitiator that upon exposure to a light source (e.g. UV light) are subjected to a process called photopolymerisation, where monomers/oligomers cross-link resulting in hardening of the object (76, 77). Ionic crosslinking is also employed to achieve solidification, the most common example is the application of calcium chloride as a solution on 3D printed objects made of alginate (78). An alternative approach is found in the use of materials that undergo chemical reactions when they come into contact with each other. These materials can be printed in a coordinated fashion creating a solid structure without the need for further processing (79). Since these strategies are the least common in the pharmaceutical arena, and therefore there are not many examples of research works that have employed them, this review will mainly focus on the first two approaches described (use of heat or solvents).

3. Rheological properties of the materials

The feasibility of transforming a 3D design into a 3D object strongly depends on the rheological features of the material to be printed. Despite the agreement on this general statement, there is still a lack of knowledge on how to screen the materials and what limits can be set as references for the viscoelastic properties. The wide variety of 3D printing technologies, the great number of applications and the big list of potential materials make the task even more difficult (80). Rheological properties are critical to design fidelity. They may depend on product quality attributes such as drug content and drug crystallinity, but at the same time, adequate rheological properties may determine the homogeneous distribution of the drug and even the crystalline state. Knowledge about the material requirements for SSE 3DP is still limited (81, 82), and most information is derived from trial-and-error approaches. The 3DP process involves processing steps that demand from the material unique and somehow contradictory rheological performances. In a simplified overview of the process, three main steps can be highlighted and qualitatively described as follows (Figure 2):

i) The material contained in a barrel or syringe should be delivered through a nozzle of a given diameter at a constant flow to obtain continuous deposition of a homogeneous strand. This step requires material flow when a pressure is applied on the barrel or syringe, but not before. Also, relevantly, no material should be extruded when the pressure is stopped. The feasibility of having a certain flow under a laminar regimen is mostly determined by the loss modulus (G'', or viscosity) of the material. It should exhibit high viscosity during rest (i.e. inside the barrel), flowability (viscosity drop) under a reasonable shear stress through the nozzle, and a rapid recovery of the viscosity to avoid further flow once deposited on the platform. Ideally, this performance demands shear thinning behaviour without thixotropy, i.e. a rapid recovery of the initial consistency in a few seconds. The viscosity of the 1st layer should be completely restored before the 2nd layer is deposited to avoid the collapse of the growing 3D object. Such a rapid restoration of the material network properties can be achieved by an adequate balance between the loss modulus (that determines the flow properties) and the storage modulus (G', determines the elastic and immediate recovery), which can be quantified using the parameter tan δ (=G''/G').

ii) The material strand should maintain the cylindrical shape of the nozzle. This feature is directly linked to the balance of G''/G' moduli described above. Objects that demand high resolution, as in the case of pharmaceutical dosage forms, require the use of nozzles with diameters in the range of a few hundred micrometres. Therefore, the material component size (e.g. insoluble fillers or crystalline drug particles) should be at least ten times smaller than that of the nozzle diameter to avoid obstruction (67). The shape of the material strand is given by the section geometry of the nozzle, and thus the extrudate must deform and adopt such a geometry, and such a change should be retained. If G' is too high, the stress stored as elastic deformation during the transit through the nozzle may be released in the exit point causing the swelling of the strand. Alternatively, when the viscous component predominates, the recovery of the viscosity after shearing due to the component's re-entanglement may cause shrinking. Therefore, for valid translation of data obtained in the rheometer to the in-situ performance in the 3D printer, the gap in the rheometer and the

diameter of the nozzle should be similar. The experiment settings should simulate the high shear stress generated at the tip of the nozzle during extrusion and subsequently at rest to fully characterize the self-healing properties of the extruded material. Nevertheless, prediction of the magnitude of swelling/shrinking of the nozzle extrudate is still a challenge (83).

iii) The strands should support the weight of further layers and act as bridges between adjacent strands of lower layers. In the manufacture of 3D printed dosage forms, the infill percentage can be modified to obtain printlets with different mechanical properties and different release profiles (84). However, 100% infill is uncommon in most biomedical applications since a certain porosity aids regulation of the release profiles of active substances and the interaction with proteins and cells. Object fidelity demands that the strands do not comb more than ¼ of their diameter in the middle of the bridge (85). Therefore, the deposited material should perform as a spring that barely deforms under the action of gravity. This demands a relevant G'. It should be noted that many attempts to prepare 3D printed foods and mortar-based constructions have failed due to residual stresses at the deposited layers, which deform the structure of the printed object (86, 87). The pressure induced by self-weight can be estimated as $\tau=\rho gh$, where ρ is the material density, g the gravitational constant and h the height of the layer. Similarly, the pressure induced by the weight of multiple layers can be inferred as as $\tau=\rho gH/\sqrt{3}$, where H is the total height of cumulative upper layers (87).

In this simplified view of the 3DP process, other non-rheology dependent factors also participate, such as the interface tension of the platform and the material, which should be high to avoid the lateral spread of the material and to maintain the circular section of the strand. The rate of drying, cooling or curing of the material should also be rapid to contribute to the hardness of the material without causing uncontrolled contractions.

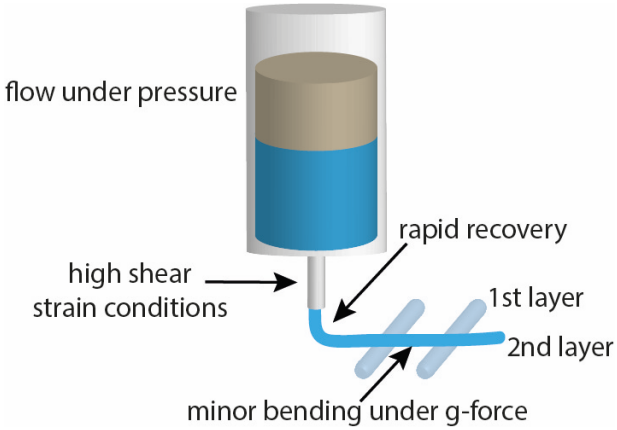

Figure 2. Schematic diagram of material extrusion through a nozzle under pressure and the rheological challenges that should be overcome.

Overall, to fulfil the main three rheological requirements described above, an ideal material should be highly structured in the barrel/syringe with the components entangled and thus showing high viscosity but also G' ≥ G'' (*tan* $\delta \leq 1$). Under the high shear strain conditions at the tip of the nozzle, the intermolecular bonds should be destroyed and the material should exhibit not only a decrease in the viscosity and G'' but also a decrease in G' of higher magnitude. Values of *tan* δ above 1 have been shown to favor flow and formation of section stable strands at the nozzle tip. After deposition, the rapid restructuring of the strand components must lead to an increase in viscosity and to even faster increment in G' with respect to G'', decreasing *tan* δ values. This enhances the self-supportiveness and mechanical strength of the material. Thus, SSE 3DP requires the material to be extrudable and self-supportable (88).

Most reports have focused on shear rate tests to characterize the shear-thinning features of the extrusion materials, and less attention has been paid to the viscoelastic properties. For example, gels of gelatin and cellulose nanocrystals were subjected to a shear rate of 0.1 s^{-1} for 60 s (in a barrel), 100 s^{-1} for 10 s (flow through nozzle) and then 0.1 s^{-1} for 60 s (after extrusion) (83). The best performing mixture showed a drop in viscosity from 838 Pa·s to 6.7 Pa·s under high shear rate conditions. The viscosity rose to 718 Pa·s at 30 s after the shear rate was minimized; namely, the gels required 30 s to recover 85.7% viscosity. When a fixed nozzle size of 0.21 mm diameter was used, extruded strands showed remarkably larger diameters (from 0.6 to 1.4 mm) as the printing temperature was increased from 5 to 25 ºC. This finding was attributed to the fact that an increase in

temperature facilitates the relative movement of the components, which in consequence decreased the viscosity more. Temperature-dependent rheological properties may facilitate the printing since a temperature induced weakness of intermolecular bonds at the nozzle contributes to a decrease in the viscosity and G' with respect to G''. The behavior of pea protein paste, alginate gel solution and their mixtures has been evaluated at a constant strain of 0.01%, heating from 25 to 85 ºC and subsequent cooling to 25 ºC (86). Mixtures exhibiting G' values close to 1000 Pa and G'' values above 500 Pa at 45 ºC, and showing strong shear-thinning behavior (viscosity drop from 6773 Pa·s to <1000 Pa·s) created objects with the highest fidelity.

Rheological analysis of drug-loaded materials before 3DP are still scarce. Mixtures of hydroxypropyl methylcellulose (HPMC, METOLOSE 90SH-100000SRm HPMC2208 type) 1 and 2 % gel with mannitol, PEG4000 and Kollidon were investigated to prepare printlets of naftopidil (10 mm in diameter, 1 mm thickness, 50% fill density) (66). The criterion used to screen the materials as a function of shear rate in the 0.01 to 100 s^{-1} was the mass with a high yield value without further analysis. A more detailed study was carried out using Carbopol 974 gels that incorporated a powder mixture of diclofenac sodium, lactose (soluble filler), Avicel PH101 and PH105 (insoluble fillers), polyplasdone (disintegrant) and glycerol (plasticizer) (82). Creep, recovery and critical strain tests revealed that an increase in the soluble components allowed for a faster flow during printing, while swellable components increased the material elastic component and exhibited higher elastic recovery after printing. However, no conclusion on the effects of the rheological parameters on the printlet quality was drawn.

Recently, a direct correlation between mechanical properties, reproducible printability and fidelity of the obtained printlets was found for HPMC (Methocel F4M) gels mixed with croscarmellose sodium (Ac-Di-Sol® SD-711) and hydroxypropyl-β-cyclodextrin (HP-β-CD; fixed content 72.1% w/w), and loaded with carbamazepine at a fixed proportion of 24% w/w (89). The printability of the material was optimized by following the rheological behavior as a function of the relative proportions of HPMC and Ac-Di-Sol® SD-711 and the volume of solvent (ethanol:water 10:90 % v/v). Orodispersible (flash) printlets were designed containing HPMC F4M 1.4% w/w and Ac-Di-Sol® SD-711 2.5% w/w (formulation I), while immediate release printlets were designed with HPMC F4M 3.9% w/w as the only gel component (formulation II). As

depicted in Figure 3, the rheological test consisted of five steps in amplitude sweep mode at 1 Hz: i) 0.5% shear strain for 300 s; ii) 100% shear strain for 120 s; iii) 0.5% shear strain for 300 s; iv) 100% shear strain for 120 s; and v) 0.5% shear strain for 300 s. The materials suitable for SSE 3DP showed self-healing features. At near rest conditions (i), they exhibited balanced viscoelasticity with G' values similar to those of G''. Under a high shear strain (ii), the materials underwent a brusque decrease in both moduli, but more remarkably in G', which means that the viscous component (G'') predominates over the elastic component (G') during extrusion from the nozzle tip. Once the strain ceased (iii), the materials progressively recovered the G' and G'' values. Interestingly, in the absence of Ac-Di-Sol® SD-711 (formulation II), there was greater and faster recovery. The rheological tests also evidenced how a minor change in the wetting of the materials could lead to the failure of the 3DP process. In formulation I, under-wetting caused the material to become too hard (higher G' and G'' values) and the flow was not sufficiently homogeneous under the pressure of the piston. On the contrary, over-wetting decreased the material G' values and delayed the recovery. Therefore, rheological assessment of the material before 3DP may be useful for quality control of successive batches, as also demonstrated for formulation II (89).

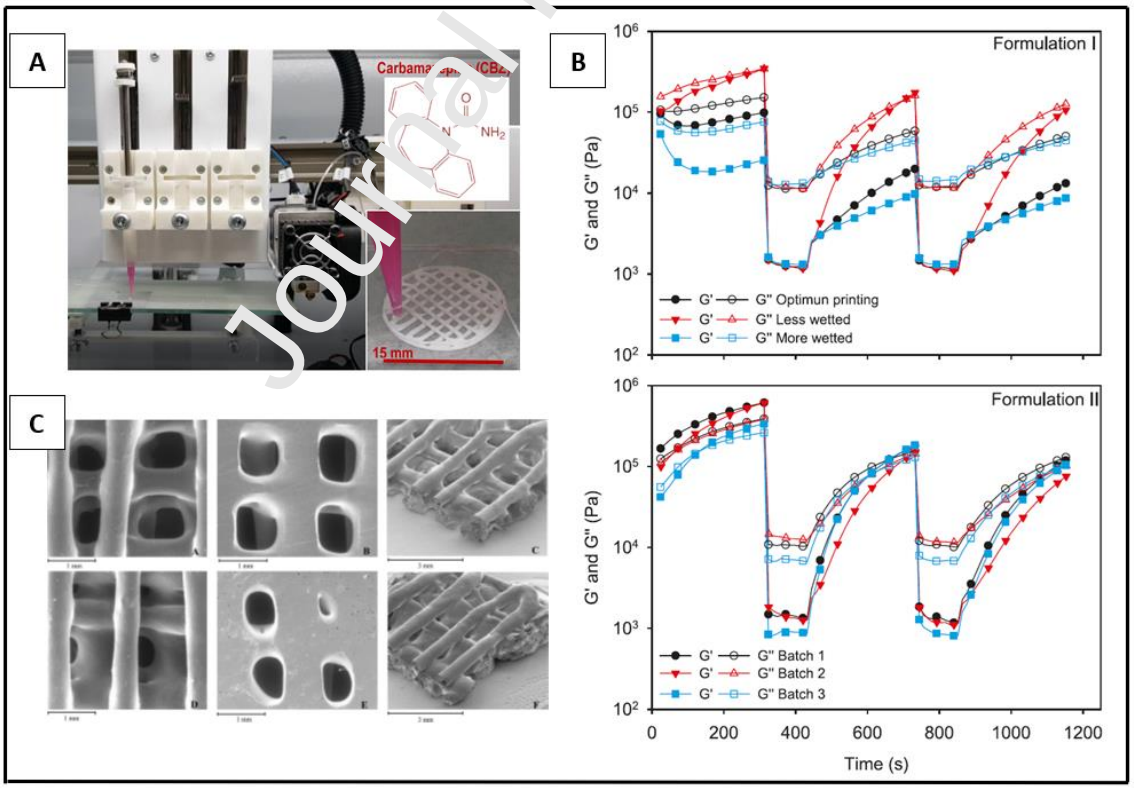

Figure 3. (A) SSE of a carbamazepine-loaded material to prepare printlets of 15 mm diameter, 3 mm height, with a diagonal (45°) infill pattern. (B) Rheological behaviour

of formulations I and II, which differ in the relative proportions of HPMC and Ac-Di-Sol® SD-711 and the volume of solvent (ethanol:water 10:90 % v/v) added. (C) SEM images of formulation I (A-C) and II (D-F) printlets (89).

It is interesting to note that the printability region for cellulose ether-based materials occurred for G' values in the region of 10^4-10^5 Pa at rest, which is in the 10^3-10^5 Pa interval found as suitable by other authors testing pastes or bioinks containing dispersed colloidal components (90-93). Therefore, such a G' value interval together with shear-thinning behavior may be used as the first tentative targets to reach when preparing drug-loaded soft materials for SSE 3DP.

4. Pharmaceutical applications of SSE 3DP

The use of SSE 3DP in pharmaceutics offers the possibility of creating complex dosage forms whilst avoiding the potentially harsh conditions sometimes associated with other printing techniques (e.g. FDM) (94). The nature of the feedstock material allows the extrusion process to be carried out at low temperatures without compromising the accuracy, and the use of pre-loaded and disposable cartridges facilitates the entire process (95). First used to produce polypills and tablets, this technology has rapidly evolved to manufacture other types of dosage forms and medical devices, from chewable tablets (59) and orodispersible films (96), to rectal suppositories (20) and implantable patches (97) (Table 1).

Table 1. Examples of dosage forms and medical devices produced by SSE 3DP

Formulation type	Formulation details/Properties	API	Excipients	Ref.
Polypill	An osmotic pump and sustained release compartments	Captopril (18.5%), nifedipine (10.7%) and glipizide (3.5%)	Cellulose acetate, D-mannitol, PEG 6000, MCC, sodium starch glycolate and HPMC	(98)
	Combination of five different drugs via two release mechanisms	Pravastatin (20%), atenolol (30%), ramipril (15%), aspirin (28.62%) and hydrochlorothiazide (5.86%)	Cellulose acetate, D-mannitol, PEG 6000, sodium starch glycolate and PVP	(75)
	Three different drugs with programmed release profiles	Metformin hydrochloride, glyburide and acarbose (ND%)	Pluronic F-127	(99)
	Controlled release fixed dose	Efavirenz (25.5%),	Brown humic acid sodium	(100)

	combination comprising of three anti-HIV-1 drugs	tenofovir disoproxil fumarate (12.8%) and emtricitabine (8.52%)	salt, hydroxyethylcellulose ethoxylate, quaternized and cellulose acetate phthalate	
Immediate release tablets	Immediate release tablets	Levetiracetam (ND%)	Polyvinyl alcohol-polyethylene glycol graft copolymer (PVA-PEG) and Polyvinylpyrrolidonevinyl acetate copolymer (PVP-PVAc)	(43)
	Immediate release tablets	Levetiracetam (ND%)	Polyvinyl alcohol-polyethylene glycol graft copolymer (PVA-PEG), Kollicoat IR	(44)
	Subdivided printlets as an alternative to the splitting of conventional tablets	Spironolactone and hydrochlorothiazide (ND%)	Lactose, corn starch, MCC, HPMC, sucrose and dextrin	(101)
	Immediate release tablets	Carbamazepine (24%)	Hydroxypropyl-β-cyclodextrin, HPMC, PVP, sodium carboxymethylcellulose and croscarmellose sodium	(89)
	Immediate release tablets	Puerarin (ND%)	PEG 4000	(49)
	Printlets fabricated with two-component cross-linkable gels	Prednisolone and bovine serum albumin (ND%)	Four-armed polyethylene glycol (PEG_4) and ε-caprolactone monomer (CL)	(79)
	Immediate release tablets with high drug loadings	Paracetamol (80%)	Croscarmellose sodium and PVP	(102)
	Immediate release tablets with high drug loadings in different geometries	Levetiracetam (96%)	Croscarmellose sodium and hydroxypropyl cellulose (HPC)	(103)
	Immediate release tablets with different volumes	Levetiracetam (93%)	Carboxymethylcellulose sodium, croscarmellose sodium and PVP	(104)
	Immediate-release formulations using thermosensitive gelatin pastes	Ibuprofen (10%)	Gelatin, glycerine, MCC, mannitol, lactose and HPMC	(105)
Controlled release tablets	Controlled release bilayer tablets	Guaifenesin (81%)	HPMC, sodium starch glycolate and MCC	(106)
	Tablets with different composition and dissolution profiles	Naftodipil (20%)	HPMC, mannitol, PEG 4000 and Kollidon CL-F	(66)
	Semi-solid tablets	Theophylline (5.36%, 7.14% or 8.93%)	HPMC 4KM and 4EM	(107)
	Tablets with pre-designed structures	Glipizide (1.7%, 2%, 2.3%)	HPMC, lactose, MCC and PVP	(108)
	Gastro-floating tablets	Dipyridamole (8.5%, 7.25%, 6.5%)	HPMC, MCC, lactose and PVP	(109)
	Floating sustained-release	Ricobendazole	Gelucire 50/13	(50)

	systems	(ND%)		
	Printable formulations after several days of storage	Levetiracetam (23.4%)	PVA-PVP copolymer, HPMC and silicon dioxide	(95)
	Sustained-release formulations using thermosensitive gelatin pastes	Diclofenac (6.45%)	Gelatin, glycerine, MCC, mannitol, lactose and HPMC	(105)
Chewable printlets	Clinical study, printlets prepared in a hospital setting with various flavours, colours, doses, and sizes	Isoleucine (ND%)	Sucrose, pectin and maltodextrin	(59)
	Chocolate-based printlets in different shapes resembling cartoon characters	Paracetamol and ibuprofen (ND%)	Bitter chocolate and corn syrup	(110)
	Lego™-like chewable bricks	Paracetamol and ibuprofen (ND%)	Locust bean gum and glycerol	(111)
	Gummies	Lamotrigine (ND%)	HPMC and gelatin	(23)
	Gummies	Ranitidine hydrochloride (ND%)	Corn starch, carrageenan, xanthan gum, gelatine	(93)
Orodispersible films (ODFs)	ODFs fabricated in a one-step-process using disposable syringes	Warfarin (1.3%)	HPC and PVA	(112)
	To develop a platform to support the extemporaneous production of ODFs	Levocetirizine hydrochloride (ND%)	Glycerine, glycine and titanium dioxide	(24)
	Multi-layered ODFs fabricated with in-process drying	Benzydamine hydrochloride (ND%)	Hydroxyethylcelulose (HEC) of different viscosity grades	(96)
	ODFs	Paracetamol (37.5%, 25% and 12.5%)	Maltodextrins with a dextrose equivalent equal to 6 and 12	(52)
	ODFs	Olanzapine (5%)	PEO, Kollidon VA 64, poloxamer 407 and poloxamer 188	(53)
	ODFs prepared in a hospital setting in comparison with the established compounded formulations	Warfarin (1.5%)	Lactose monohydrate, HPC and propylene glycol (PG)	(113)
	ODFs for veterinary use	Prednisolone (1%)	PEO, HPC, pure liver powder	(114)
Solid self-emulsifying formulations	Solid self-microemulsifying printlets in various geometries	Fenofibrate (7%) and cinnarizine (7%)	Gelucire 44/14, Gelucire 48/16 and Kolliphor	(71)
	Solid lipid tablets	Fenofibrate (ND%)	Maisine CC, Captex 355 EP/NF, Capmul MCM EP, Soybean oil, Kolliphor EL, Tween 85 and methyl cellulose	(115)
	Self-emulsifying suppositories prepared in different sizes without the aid	Tacrolimus (0.12%)	Gelucire 44/14, Gelucire 48/16 and coconut oil	(20)

	of moulds			
	Self-emulsifying suppositories with a size adapted for administration to rats	Tacrolimus (0.9%)	Gelucire 44/14 and coconut oil	(22)
Medical devices	Devices cured with UV light	Prednisolone (0.5%, 1% and 1.5%)	Silopren UV LSR 2030	(77)
	Patches	5-fluorouracil (ND%)	Poly(lactic-co-glycolic acid) PLGA and polycaprolactone (PCL)	(97)
	Hydrogel patches	Doxorubicin (ND%)	Semi-synthesized fish gelatin methacryloyl (F-GelMA), carboxymethyl cellulose sodium (CMC)	(116)
	Microneedles	Insulin (ND%)	Alginate, hydroxyapatite, calcium chloride	(78)
	Biopierces	Mupirocin (20%, 30% and 40%)	PLGA	(117)
	Patches	Propolis (56%)	Pectin from apple and β-cyclodextrin	(118)

*ND% (not clearly disclosed %)

4.1.Polypills

Polypills combine multiple active pharmaceutical ingredients (APIs) in one dosage form (Table 1) (119). SSE 3DP has been applied to the production of polypills containing multiple drugs in individual compartments, to obtain different release profiles for each drug. This is the case for a polypill that incorporates nifedipine and captopril (both used to treat arterial hypertension in type II diabetes) and glipizide (treatment for type II diabetes) (Figure 4A) (98). Incorporating all three drugs into the same solid dosage form would be highly beneficial in treating diabetic patients, however, the formulation would require distinctive and independent release profiles for each drug. To do so, captopril was included in a compartment encapsulated by a porous cellulose acetate shell to restrict drug release through osmosis, resulting in a zero-order release profile. Both nifedipine and glipizide were enclosed in two different compartments which were encapsulated in the porous shell on all but the superior face to enable release of the drug by diffusion, resulting in a first order release profile. Moreover, a HPMC hydrophilic matrix was employed to reduce the drug release for both nifedipine and glipizide. In contact with aqueous liquid, HPMC swells and forms a viscous gel that acts as a diffusion barrier, inhibiting water from reaching the drugs.

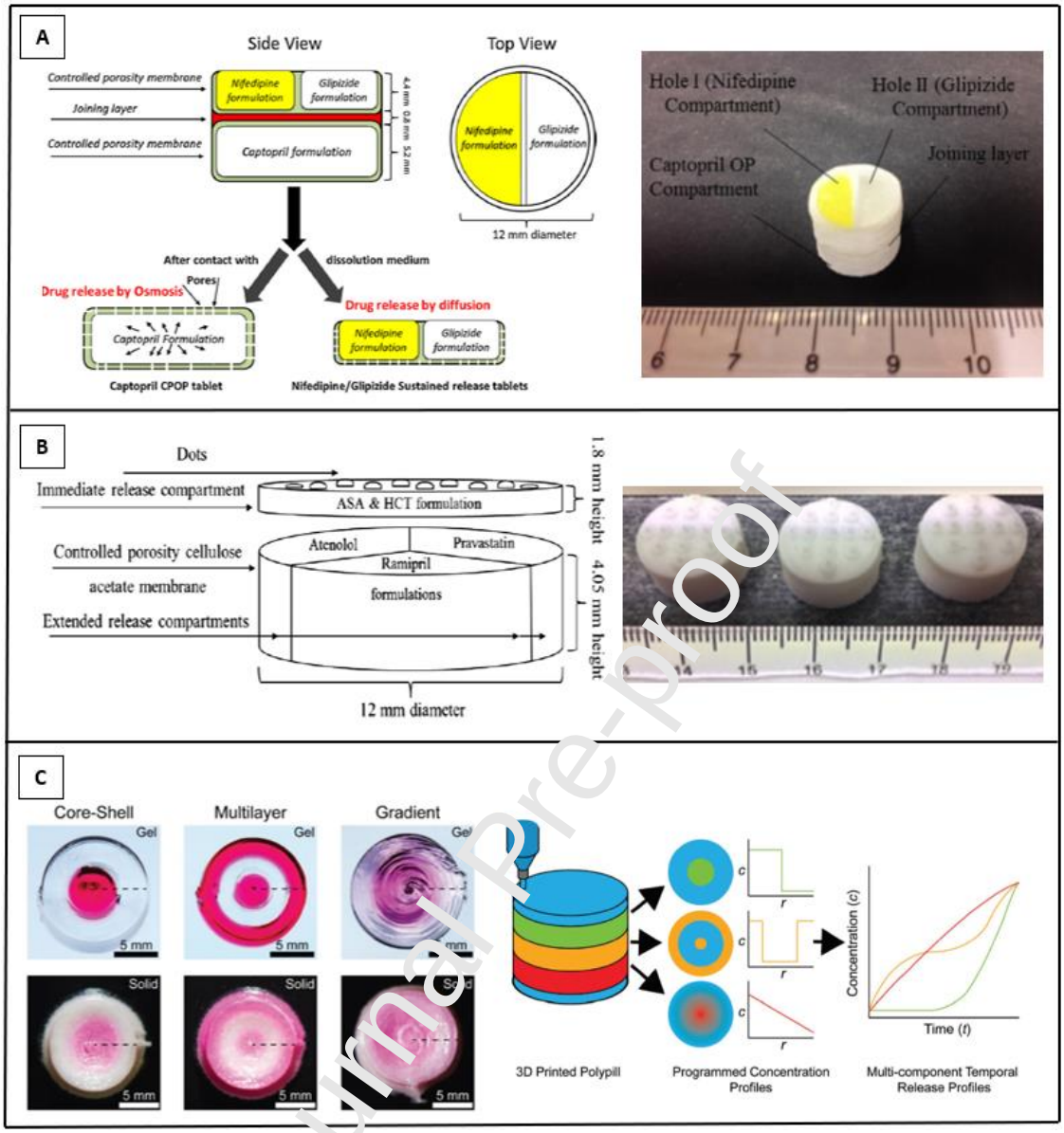

Figure 4. (A) On the left, schematic diagram of a polypill containing three different drugs separated into different compartments with different release mechanisms and on the right, a photograph of the printed polypill (98). (B) On the left, a schematic diagram of the polypill design; above, the immediate release compartment and below the three sustained release compartments and on the right, a photograph of the printed polypills (75). (C) On the left, top-down photographs of the 3D printed hydrogel Pluronic F-127 polypills containing core–shell, multilayer, and gradient concentration profiles acquired after the 90 min processing interval. A red dye facilitates the measurement of the radial concentration profile using image processing techniques and below, top-down photographs of the same 3D printed Pluronic F-127 polypills acquired after the 12 h post-processing interval. On the right, a schematic figure showing the concept of programming temporal release profiles of individual actives from a single polypill by

controlling their spatial distributions (99). Figures reproduced and modified with permission from (75, 98, 99).

The same approach has been applied to fabricate a polypill containing five different drugs with two independent release profiles (Figure 4B) (75). The polypill was aimed to treat cardiovascular pathologies that require the intake of multiple tablets by patients. It was comprised of an immediate release compartment with aspirin and hydrochlorothiazide and three sustained release compartments that contained atenolol, pravastatin and ramipril. As in the study described above, a cellulose acetate shell was also employed in this work to contain the active drugs, in this case atenolol, pravastatin and ramipril, which were also mixed with a hydrophilic matrix formed by HPMC. Aspirin and hydrochlorothiazide mixed with a disintegrant were extruded on top of the sustained release compartments, forming a separate immediate release compartment. Finally, dots were printed on the surface of the polypill to facilitate identification.

SSE 3DP was also utilised to produce a polypill containing three drugs used for the treatment of type II diabetes (metformin hydrochloride, glyburide and acarbose) (99). Pluronic F-127 was selected as an excipient due to its ability to form free-standing hydrogel structures. The drug-loaded hydrogel was printed with three different spatial distributions of the drugs within the polypill, these being core-shell, multilayer, and gradient structures. These three concentration profiles generated delayed, pulsed, and constant release profiles, respectively, that can be maintained for at least 5 hours. However, the study of mass transfer processes showed that the programmed concentration profiles changed throughout the processing and post-processing intervals. This means that the concentration profiles obtained after pill shrinkage and solidification did not match the programmed structures, although the photographs shown in Figure 4C suggested that the programmed distributions persisted after the post-processing interval. The level of complexity achieved in such polypills would be difficult to attain with conventional tablet manufacturing processes. SSE 3DP provides a suitable solution, given its ability to extrude multiple feedstocks at the same time.

SSE 3DP was used to prepare a tri-therapeutic tablet matrix that included three anti-HIV-1 drugs (efavirenz, tenofovir disoproxil fumarate and emtricitabine) (100). Humic acid-polyquaternium 10 complex (HA-PQ10) was used as the polyelectrolyte

framework to achieve controlled drug release. The 3D printed formulations were assessed *in vivo* in a pig model and compared with the commercial tablet (Atripla®). Sustained drug release within the therapeutic index was obtained for the 3D printed tablets, with improved relative bioavailability of all three drugs compared to the conventional formulation.

4.2. Tablets

SSE 3DP is being widely applied in the field of tablet manufacturing. 3D printed tablets (also known as Printlets™) can be produced to avoid swallowing (chewable printlets), with different release profiles (e.g. immediate or controlled release), or with unique characteristics (e.g. high-drug loadings) that can be tailored to each patient's needs.

4.2.1. Immediate release tablets

SSE 3DP has demonstrated to be a suitable technology to produce immediate release tablets (Table 1). An important benefit that 3DP brings to drug manufacture is the possibility to tailor treatments to the requirements of each patient. Such is the case in a study that prepared immediate release levetiracetam tablets (43). Levetiracetam is used to treat epilepsy, where the dose in paediatric patients is subsequently increased over the weeks. Thus, this work takes advantage of the flexibility offered by 3DP to prepare tablets that can be easily modified to follow the required dosage regimen. The tablets released the drug between 10-20 minutes, depending on the excipients employed; the use of organic solvents, generally used to prevent clogging of the printer nozzle, were avoided. In a subsequent work, levetiracetam tablets with different numbers of layers were prepared to mimic different doses for paediatric subgroups (44). The drug dissolution was dependent of the number of layers and an increase in the number of layers resulted in a decrease of the drug release rate. However, all formulations disintegrated within 3 min, thus complying with the requirements of the European Pharmacopeia. Moreover, SSE 3DP was also employed to prepare subdivided tablets of spironolactone and hydrochlorothiazide as an alternative to conventional subdivided tablets by manual splitting (101). The 3D printed tablets were superior to the split ones in terms of drug content and mass variation and complied with the European Pharmacopeia specifications.

Cyclodextrins, oligosaccharides widely used in pharmaceutics to increase drug solubility, were used as hydrophilic fillers to prepare orodispersible and immediate release carbamazepine printlets (Figure 5A) (89). Both formulations were able to completely release the drug in less than 60 min, a faster release compared to the dissolution profile of the drug in powder form, highlighting the beneficial effect of cyclodextrins on drug solubility. Besides cyclodextrins, other excipients have been explored to act as a suitable matrix for the fabrication of rapid-release tablets. For instance, polyethylene glycol (PEG) 4000, a polymer often employed to prepare solid dispersions due to its low melting point, was used to prepare immediate release tablets loaded with puerarin (49). PEG 4000 is not used in direct powder compression for tablet manufacturing due to its adhesive behaviour but has been proven to be suitable for 3DP of solid dosage forms. Moreover, the possibility of extruding two copolymers in a coordinated fashion to react with each other and form the printlet has also been explored (79). The pre-polymer used was a combination of a four-armed PEG with a pentaerythritol core polycaprolactone (PEG_4-PCL), which was subsequently functionalised with N,N-disuccinimidyl carbonate (PEG_4-PCL-SC) or with amine groups (PEG_4-PCL-NH_2). The two copolymers underwent a cross-linking reaction upon contact that formed a stiff gel, capable of forming an object without the need for solvents, UV irradiation or heat.

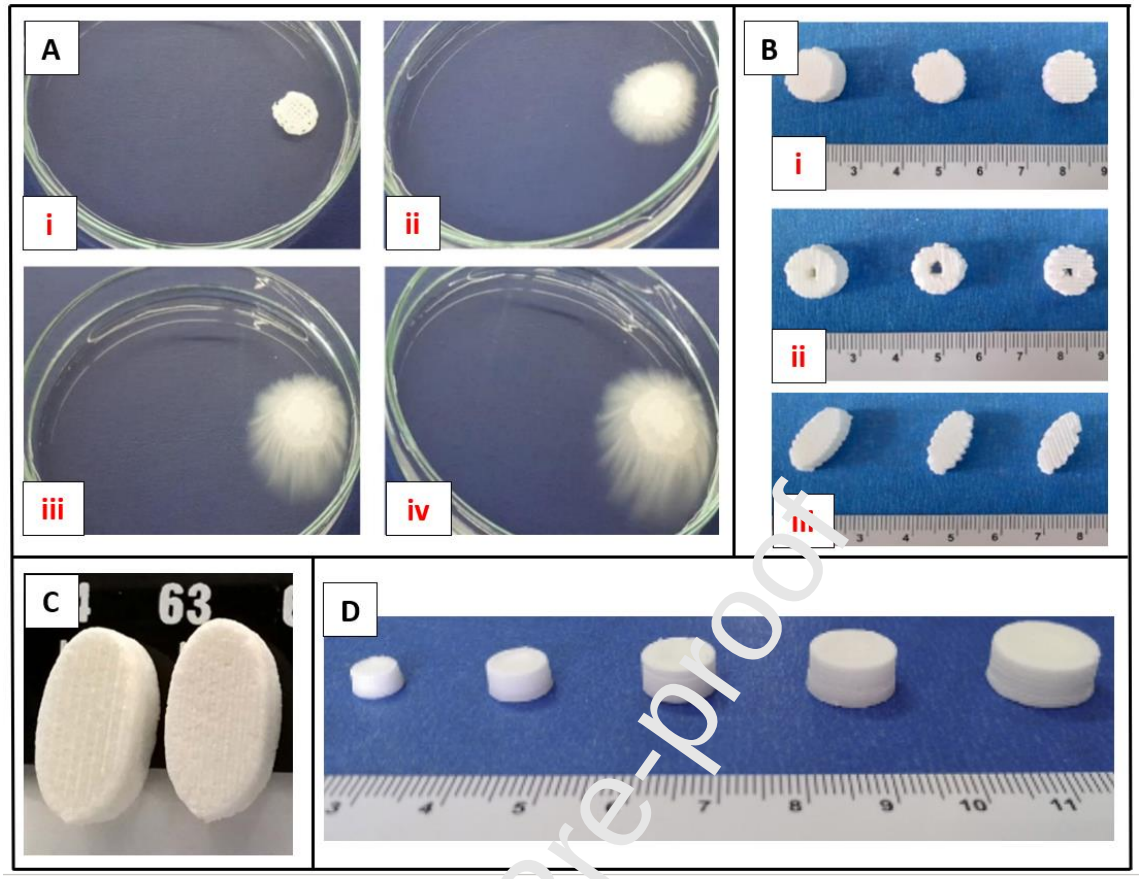

Figure 5. (A) Disintegration of a carbamazepine printlet in a Petri dish containing distilled water after: i) 5 s; ii) 120 s; iii) 360 s; and iv) 540 s (89). (B) Levetiracetam loaded printlets in three different shapes (cylinder (i), torus (ii) and oval (iii)) (103). (C) Photograph of immediate release tablets loaded with paracetamol (102). (D) Side view of levetiracetam printlets with increasing volumes (104). Figures reproduced and modified with permission from (89, 102-104).

Furthermore, the manufacture of immediate release tablets with high drug loads is also possible using SSE 3DP, as demonstrated for paracetamol tablets with drug loads of up to 80% (w/w) (Figure 5C). These tablets were able to release at least 90% of the drug within 10 min and their physical and mechanical properties were within the standards of the United States Pharmacopoeia (USP) (102). Another example of the high drug loads that can be achieved using SSE can be found in a work in which levetiracetam tablets with a drug load of 96% (w/w) were prepared (Figure 5B) (103). The tablets were prepared in different geometries (cylinder, torus and oval), obtaining in almost all cases a drug release of more than 85% within 15 min. However, the fastest drug release (97.45% within 2 min) was achieved with the torus-shaped tablets of 50% infill. Other

work has also used levetiracetam to prepare immediate release tablets, but through manipulation of the tablet volume it was possible to obtain varying drug loads (Figure 5D) (104).

4.2.2. Controlled release tablets

SSE is also capable of producing dosage forms with controlled release properties (Table 1). Controlled release bilayer tablets containing guaifenesin were prepared and then compared to commercially available bilayer tablets (106). The 3D printed tablets displayed the same initial burst release followed by a sustained release over a period of 12 h as the commercial tablets. To achieve this, the two layers were prepared using different viscosity grades of HPMC. Moreover, the highest concentration of HPMC (14%) of all tested for the sustained release layer, obtained the release profiles most similar to commercial tablets. In a different study, naftopidil tablets were prepared using hydrogel-based materials as the printing ink (66). Different amounts of HPMC hydrogels (30%, 40% and 50% gel) were incorporated into the printer ink and it was observed that the amount of HPMC hydrogel greatly affected the characteristics of the final formulation. As the amount of HPMC hydrogel was increased, a more delayed drug dissolution was obtained, and the weight and hardness of the tablets decreased. Also using HPMC as the main excipient, extended-release theophylline tablets were prepared using hydrogels made from two different types of HPMC: K4M and E4M (107). The hydrogel containing HPMC K4M (12% w/w) showed the best extrudability and shape retention ability (Figure 6A). The in vitro dissolution test showed that the drug is released from the 3D printed tablets over 12h.

The use of thermosensitive gelatin pastes to achieve different drug release patterns has also been reported (105). Gelatin is a temperature-sensitive polymer and its behaviour can be altered with the addition of certain additives. For instance, the extrusion of 30% (w/w) gelatin pastes with 25% (w/w) microcrystalline cellulose (MCC) resulted in extruded filaments with a smooth, uniform surface compared to those without MCC, demonstrating that the addition of MCC can improve the extrudability of the gelatin pastes. However, when the MCC concentration was increased from 25% to 35% (w/w) the pastes were highly viscous and had low fluidity, greatly affecting their printability. Moreover, the effect of another additive, HPMC, on the release behaviour of the

formulations was evaluated. With the increase in HPMC from 15% to 30% (w/w), the drug release lasted for a period of 24h in comparison to the 4h release obtained with the addition 15% and 20% (w/w) HPMC. Rheological studies confirmed that the addition of MCC or HPMC resulted in better shear-tinning and adequate paste viscosity, beneficial to the smooth extrusion and rapid deposition of the gelatin pastes. In addition, immediate or sustained release formulations can be obtained depending on the addition of HPMC to the gelatin matrix.

Alternatively, drug release can be modulated by changing the internal structure of the 3D printed tablets. The dissolution profiles of twelve tablets designed with different outline and grid width values showed that the structural design influenced the drug release profile (108). As the grid width increased, the drug release was greater, which can be explained by the increased surface area of the tablets that facilitated dissolution and drug diffusion (Figure 6B).

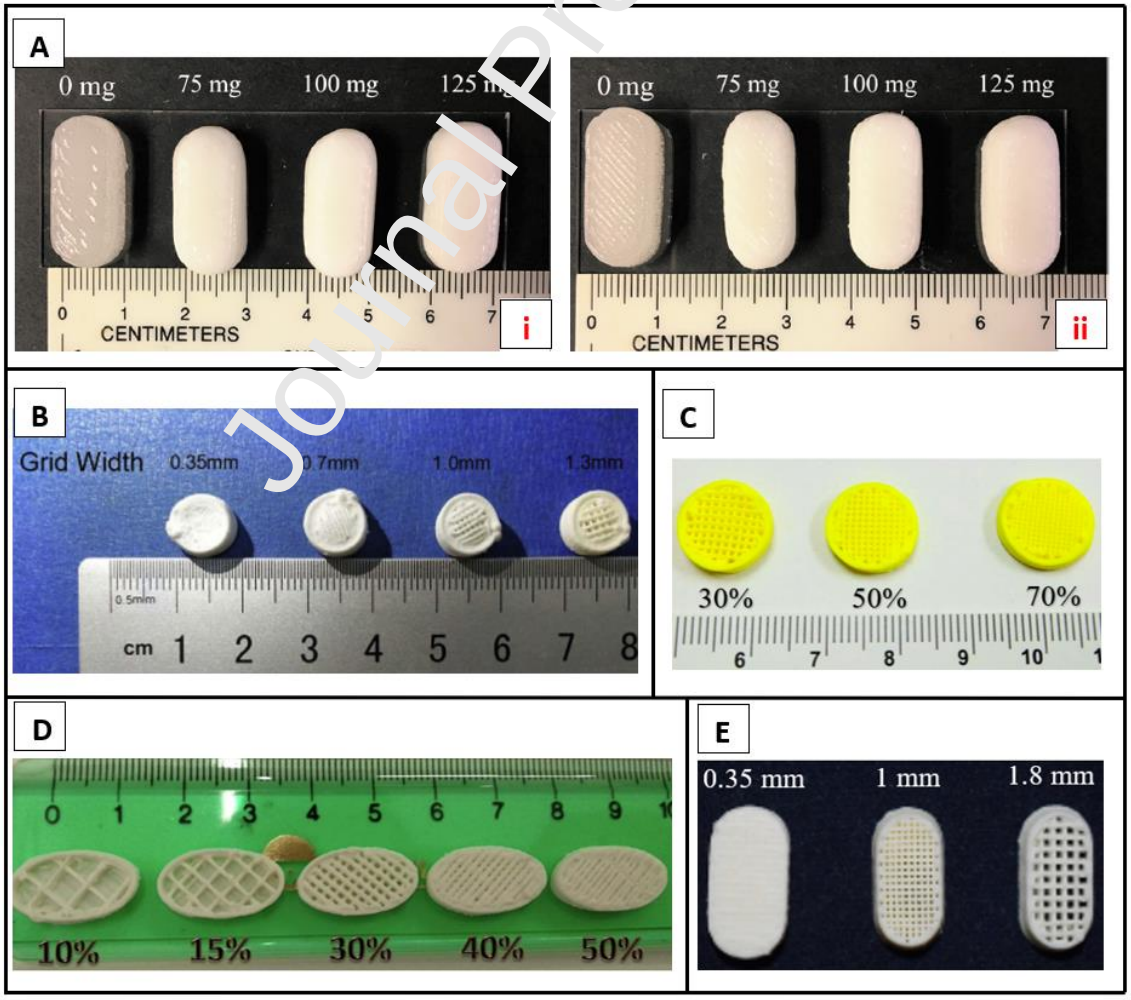

Figure 6. (A) Photographs of increasing weight 3D printed tablets made with different concentrations of HPMC 4KM: i) K4M10% and ii) K4M12% (107). (B) Image of 3D printed tablets displaying different grid width values in their structures (108). (C) 3D printed gastro-floating tablets with different infill percentages (109). (D) Floating sustained-release printlets with different fill densities (50). (E) 3D printed tablets with different infill designs and varying distances between printed strands (95). Figures reproduced and modified with permission from (50, 95, 107-109).

Gastro-retentive drug delivery systems are used to prolong the gastric residence time of drugs that, for example, are locally active in the stomach or soluble at acidic pH and unstable at basic pH (120). Using SSE, it was possible to fabricate gastro-floating tablets loaded with dipyridamole with three different infill percentages (30%, 50% and 70%) (Figure 6C) (109). The internal low-density lattice structure provided buoyancy to the tablets, and the drug release analysis showed that a sustained release profile was obtained for at least 8h. The tablets with infill percentages of 30% and 50% possessed longer float time due to their lower density and greater air encapsulation. The tablet with 50% infill achieved a perfect compromise between suitable drug release and floating time. These results open the possibility of tailoring these systems to each patient, depending on their individual variations in gastric physiology.

Floating medicines may also improve the bioavailability of some drugs with enhanced solubility in acidic environments by means of retaining the formulation in the stomach (121). Such is the case for ricobendazole, a drug employed in the treatment of parasitic diseases, whose bioavailability is further improved when it is included in lipid-based formulations. Using Gelucire 50/13, a fatty PEG ester with a low melting point and rapid solidification, it was possible to prepare floating devices loaded with ricobendazole (50). Although the authors of the study called the process “solvent-free melting solidification printing process”, the described process is the conventional SSE 3DP and the Gelucire excipients have been previously reported for the production of printlets (20, 71, 122) (Figure 6D).

A mixture of HPMC, polyvinyl acetate/polyvinylpyrrolidone copolymer (PVAc-PVP) and highly dispersed silicon dioxide (SiO_2) was used as the polymer matrix to obtain a sustained release of levetiracetam (Figure 6E) (95). Similar sustained drug release

dissolution profiles were obtained using freshly printed tablets or tablets printed from stored organic solvent free inks. Moreover, the printing formulations were analysed by X-ray powder diffraction (XRPD), showing no changes in the drug solid-state during storage.

4.3. Chewable printlets

Among the possibilities offered by this technology, the production of chewable medicines is one of the most applicable and relevant (Table 1) (59). The production of easy-to-swallow formulations could greatly improve patient acceptability, especially amongst geriatric and paediatric populations. In children, the taste, smell and viscosity are also important features that determine the acceptability of the formulation (123).

The suitability of using SSE 3DP to manufacture personalised treatments has already been reported in a study carried out in a hospital setting with paediatric patients obtaining satisfactory results (59). Chewable printlets of isoleucine in various colours and flavours were prepared as a treatment for a rare metabolic disease that mainly affects children (Figure 7A). Isoleucine blood concentrations after three months of treatment with printlets were compared to the blood levels obtained with the conventional isoleucine capsule formulation prepared by pharmaceutical compounding at the hospital. There were no significant differences between the isoleucine blood levels obtained with printlets or with the compounded formulation. However, isoleucine printlets showed less variability in drug blood concentration and were closer to the target levels. Moreover, the printlets were well accepted by the children, although each patient had their own preferences regarding colour and flavour. Thus, 3DP should be considered as a potentially novel technique to prepare compounded medicines in a cost-effective and automatic way, avoiding the common safety problems related to manual compounding such as compounding errors, which could lead to inaccurate dosing and undesirable side effects.

Figure 7. (A) Chewable isoleucine printlets prepared in different sizes, flavours and colours (59). (B) 3D printed chocolate-based dosage forms (110). (C) Side views (i and ii) and bottom (iii) of an oral Lego™-like gelatin-based dosage form of paracetamol (blue) and ibuprofen (red) (111). (D) 3D printed gummies in different shapes: heart, gummy bear and disk (93). (E) 3D printed gummies in various shapes and colours (23). Figures reproduced and modified with permission from (23, 59, 93, 110, 111).

In another study, chocolate-based dosage forms were fabricated using bitter chocolate and corn syrup as excipients (110). The formulations loaded with ibuprofen and paracetamol were printed in different shapes resembling familiar cartoon characters (Figure 7B). A variant of SSE 3DP consisting of extruding semisolids within a solidifying liquid matrix to produce Lego™-like chewable printlets was also proposed (Figure 7C) (111). Paracetamol and ibuprofen powders were suspended in a locust gum solution, forming a paste that was directly printed into a gelatin-based matrix. One advantage of this system is the possibility of encapsulating the drug paste within a

matrix that masks its flavour, as in the case of some bitter-tasting drugs. Following these strategies to make medicines more pleasant for children, 3D printed gummies were fabricated with different shapes (heart, bear and disc) using mixtures of gelatin, carrageenan, xanthan gum and sweeteners (Figure 7D). Ranitidine hydrochloride was used as model drug and it was observed that the addition of corn starch amongst the components obtained a greater extended release of the drug (93). Also using gelatin and HPMC hydrogels, gummies in different shapes and colours were prepared incorporating lamotrigine (Figure 7E) (23). The viscosity and strength of the formulations were easily modified by varying the amounts of the two main excipients, HPMC and gelatin.

4.4. Orodispersible films

Another interesting approach to improve patient acceptability of medicines in population groups with dysphagia is the preparation of orodispersible films (ODFs), especially if they can be administered without water (Table 1). Such is the case of a study in which ODFs containing warfarin, a drug used for the treatment and prevention of thromboembolic events with a narrow therapeutic index, were prepared using SSE (Figure 8A) (112). Conventional warfarin therapy is based on the administration of commercially available tablets of fixed doses, which commonly lead to tablet splitting to tailor the dose to the patient. The preparation of ODFs makes it possible to tailor the dose to each patient's requirements with the additional advantage of being especially suitable for patients with swallowing difficulties. Although geriatric patients fall into the category of dysphagia patients, the administration of ODFs to this group is generally not recommended due to the difficulties they may experience in picking up the thin ODF films.

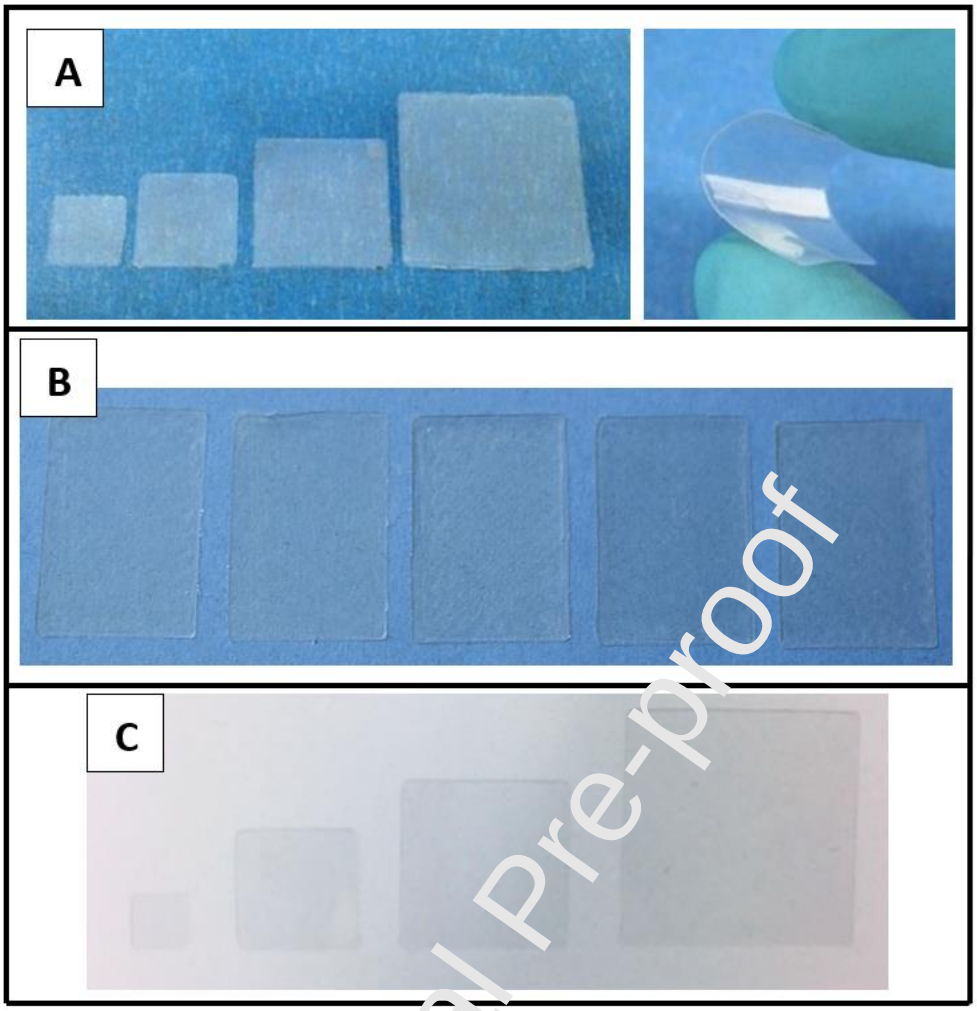

Figure 8. (A) From left to right: 25, 50, 100 and 200 mm^2 drug loaded films (112). (B) Blank ODFs, 45 to 205 µm model height (left to right) (96). (C) Warfarin-loaded ODFs in different sizes (113). Figures adapted and reproduced with permission from (96, 112, 113).

ODFs containing levocetirizine hydrochloride, a H_1-receptor agonist used to relieve symptoms of allergic rhinitis, were also fabricated using this approach (24). In children, the dose of this drug depends on the age of the patient and is commonly administered in the form of an oral solution and fixed-dose tablets. SSE allows printing ODFs with a dose tailored to each age group, avoiding the need to split commercial tablets and preventing dosing errors derived from the use of oral solutions. In another study, the possibility of implementing an in-process drying to improve the mechanical properties of the films and shorten the overall drying time was investigated (Figure 8B) (96). This was possible by adjusting the viscosity of the dispersion to be printed using hydroxyethyl cellulose (HEC) as a thickening agent. Moreover, the drug content could

be modified by changing the thickness of the film or the concentration of the drug in the print dispersion. On the other hand, simply wetting of the mixture of drug and powdered excipients with glycerine enabled the printing of the films directly on the packaging foil (52).

The concept of producing ODFs using 3DP in hospital settings as potential formulations to replace conventional compounding was explored by the preparation of warfarin loaded ODFs for paediatric patients (Figure 8C) that include QR codes containing information about the dosage form (113). The conventional formulation was composed of oral powders in unit dose sachets obtained from the crushing of commercially available tablets. Amongst the advantages shown by 3D printed ODFs, the more accurate drug content compared to conventional formulations and easier administration directly into the patient's mouth without the need for water can be highlighted. On the contrary, the powder in the unit dose sachets needs to be dissolved in a liquid before administration. Apart from children or patients with swallowing difficulties, this approach could be used to administer drugs to patients who are non-adherent, such as psychiatric patients (53), as ODFs are more difficult to purposely expel from the mouth and do not cause choking during administration.

Another interesting application of ODFs is for the administration of veterinary medicines. Since the number of approved veterinary drugs is limited, it is common to use off-label human medicines. The manufacture of prednisolone loaded ODFs for veterinary use in an animal clinical setting has set a precedent for dose personalisation for animals (114).

4.5. Solid self-emulsifying formulations

Some examples of semisolid materials that are generally used as printing inks in SSE are polymers such as PVP, polysaccharides such as cellulose, starches and gelatin. However, the feasibility of using lipid-based inks to manufacture dosage forms has been recently explored (122). Lipid-based excipients are obtained from vegetable oils, waxes or fatty acids that are widely used as suitable carriers for the delivery of poorly water soluble drugs (124). Self-emulsifying and self-micro emulsifying drug delivery systems (SEDDS and SMEDDS, respectively) represent an effective strategy to enhance the oral bioavailability of poorly soluble drugs.

In contact with aqueous media, SEDDS and SMEDDS form kinetically stable oil-in-water (O/W) emulsions or microemulsions, whereby the drug is solubilised within the small lipid droplets (125). Generally, these formulations are filled into gelatin capsules to facilitate oral administration or formulated as tablets, pellets or granules using solidifying techniques (126). However, to generate a solid dosage form, such approaches generally require a large amount of solid carriers such as cellulose and lactose, and their administration as liquid forms within the gelatin capsules may lead to stability issues. To date, there are few studies that describe the use of SEDDS or SMEDDS in 3DP. For instance, drug loaded solid-SMEDDS (S-SMEDDS) were fabricated in different geometries (cylindrical, prism, cube, and torus) without the need for a solid-phase carrier (Figure 9A) (71). The use of a refrigerated build plate facilitated the solidification of the printed strands, with only a minor slumping of the lower layers. The dispersion time of the printlets was clearly affected by the geometrical shape, with the torus having the lowest dispersion time due to its higher surface area to volume (SA/V) ratio.

A different approach is found in the preparation of solid lipid tablets based on emulsion gels (115). Unlike previous approaches where blends of lipid excipients are directly printed, these formulations are printed using preformed oil-in-water (O/W) emulsions loaded with the poorly soluble drug fenofibrate. The formulations obtained disintegrated in less than 15 min. Besides being possible to print the tablets at room temperature, which is particularly useful for thermolabile compounds, these types of formulations are especially indicated for poorly-water soluble drugs as they help to improve their oral bioavailability.

Besides oral dosage forms, lipid excipients with self-emulsifying properties can also be employed to prepare suppositories. Suppositories loaded with the immunosuppressant tacrolimus, commonly used in patients with therapy resistant inflammatory bowel disease (IBD) have already been prepared (Figure 9B) (20). Due to the lack of commercially available tacrolimus suppositories, these are commonly compounded in hospital pharmacy settings by a moulding technique, which requires several steps and long periods of solidification. Using SSE and a suitable combination of lipid excipients, self-supporting suppositories were directly printed without the aid of moulds. Moreover, the suppositories were fabricated in various sizes to suit the patient's comfort and dose

requirements. They were prepared using a mixture of Gelucire 44/14 or Gelucire 48/16 and coconut oil, the latter used as a plasticising agent. Both formulations displayed good printability properties without the need for solid-phase carriers or a cooling system in the build plate. Furthermore, both suppository types released more than 80% drug within 120 minutes. In a subsequent study, the therapeutic activity of the lipid suppositories was tested in an animal model of ulcerative colitis (22). To do so, the suppositories were adapted in size and dose for their administration to rats and PET/CT imaging was used as a non-invasive tool to monitor the disease progression. The successful results of the study highlighted the usefulness of 3DP to test the efficacy of new formulations in preclinical studies.

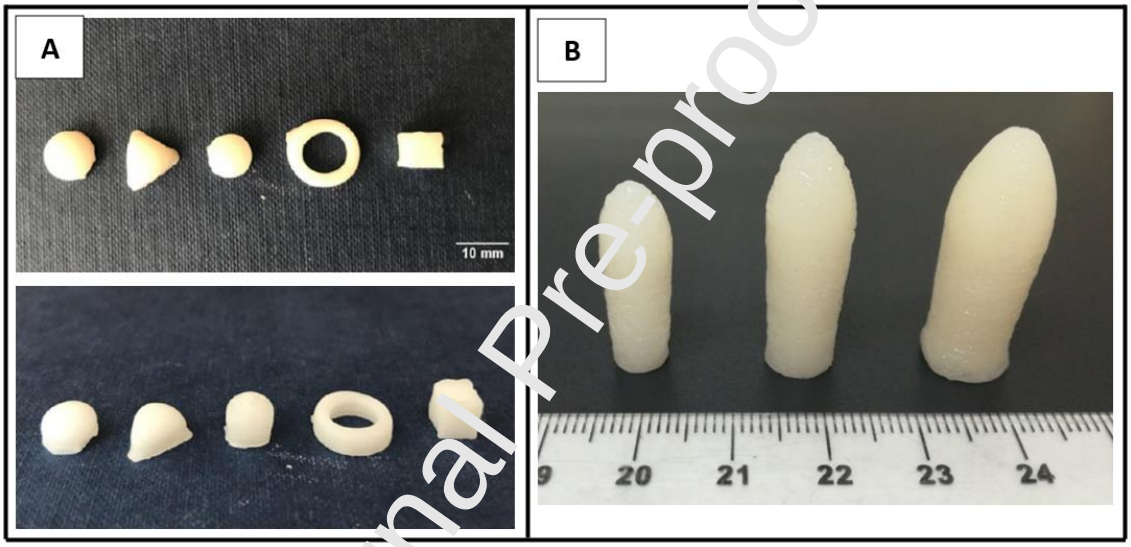

Figure 9. (A) Images of drug loaded S-SMEDDS formulations in various geometrical shapes (cylindrical, prism, cube, torus and cube) (71). (B) Lipid-based suppositories with self-emulsifying properties intended for human administration, printed in three different sizes as an example of personalisation (20). Figures adapted and reproduced with permission from (20, 71).

4.6. Drug-medical devices combination products

Although other 3DP technologies, such as vat photopolymerization (30), have been more widely applied to the production of medical devices, some examples of devices produced using SSE 3DP can also be found. For instance, polydimethylsiloxane (PDMS), a polymer widely used in reservoir devices such as implants and inserts, can be extruded at room-temperature and then crosslinked with UV light to manufacture prednisolone-loaded structures (Figure 10A) (77). Moreover, implants and patches

made by SSE have also been applied in the local treatment of some cancers showing promising results. Flexible patches incorporating high drug loadings of the anti-cancer drug 5-fluorouracil were fabricated using a blend of poly(lactide-co-glycolide) (PLGA) and polycaprolactone (PLA). The patches were found to be capable of releasing the drug over four weeks and exhibited a suppressive effect on the growth of subcutaneous pancreatic cancer xenografts in mice (Figure 10B) (97). In other work, patches for implantation in cancer tissue were prepared using a semi-synthetic fish-gelatin polymer (fish gelatin methacryloyl) and carboxymethyl cellulose sodium (CMC), in which PEGylated liposomes loaded with the drug doxorubicin were entrapped (Figure 10C) (116). The structures were fabricated in three different shapes (cylinder, torus and gridlines) and were crosslinked using UV light. The release rate of the drug from the patches was found to be dependent on the UV exposure time; the longer the devices were exposed to UV light, the more delayed the drug release.

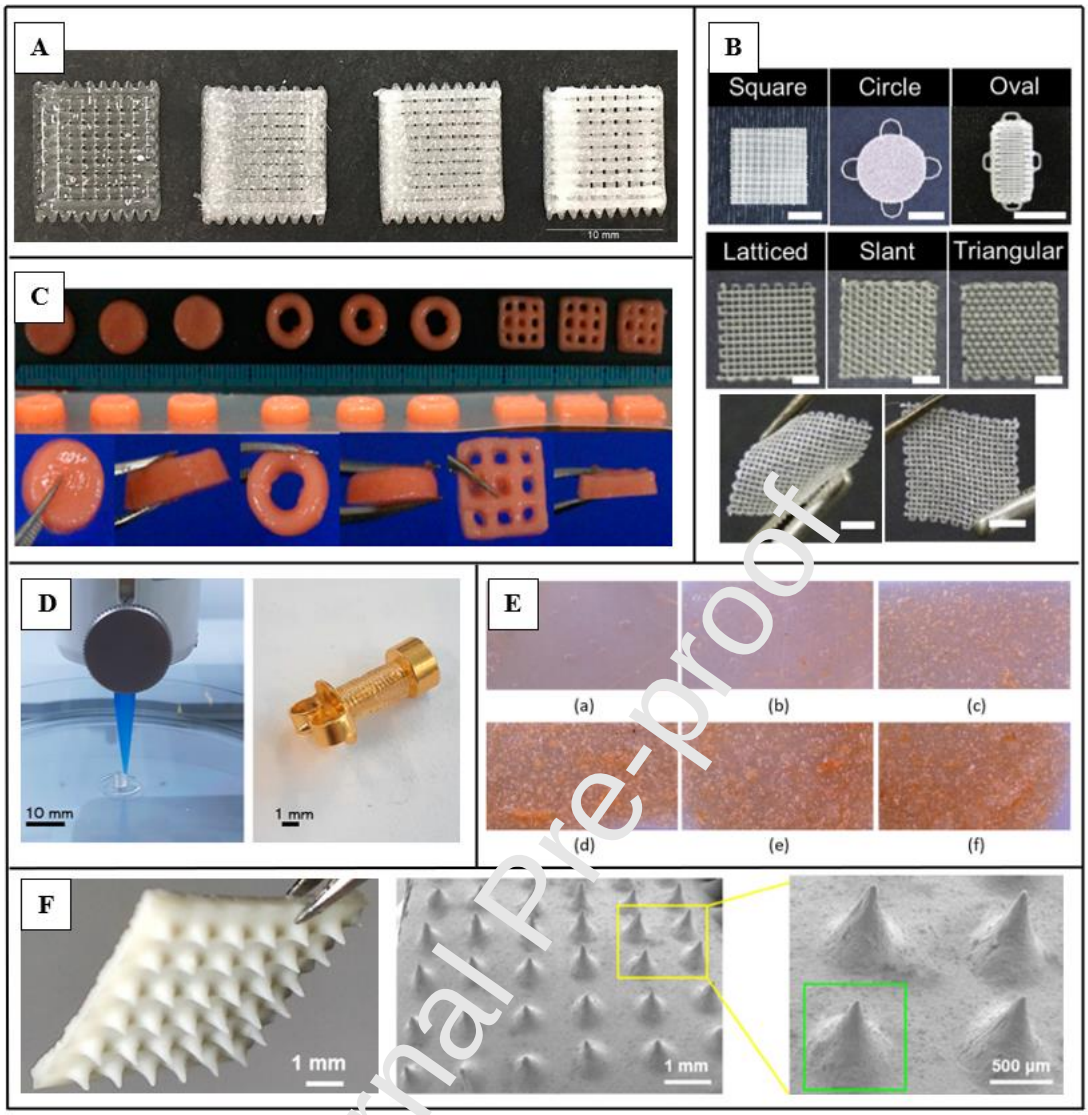

Figure 10. (A) Photographs of prednisolone-loaded structures. From left to right: placebo, 0.5%, 1.0% and 1.5% drug containing structures (77). (B) Above, 3D printed patches on different shapes (square without loops, circle and oval shapes with loops on each side for suturing). In the middle, 3D printed patches with three different types of pores (latticed, slanted, and triangular) (scale bar: 5 mm). Below, photographs demonstrating the flexible and stretchable properties of the 3D printed patches (scale bar: 2 mm) (97). (C) Images of 3D printed patches with PEGylated liposomal doxorubicin before UV irradiation (116). (D) On the left, 3D printing of the drug-eluting scaffold (biopierce). On the right, photograph of the biopierce assembled on a piercing stud (117). (E) Optical microscopy images of 3D printed pectin patches with: (a) 0%, (b) 2.5%, 5%, (c) 10%, (d) 20% and (e,f) 30% w/w chitosan and cyclodextrin/propolis extract inclusion complex particles (118). (F) On the left, photograph of 3D printed microneedle patch and on the right, SEM images of the

microneedle patch with 5 × 6 needle array and 2 × 2 needle array (78). Figures adapted and reproduced with permission from (77, 78, 97, 116-118).

An interesting application of SSE for the manufacture of medical devices is found in the creation of drug-eluting and bio-absorbable scaffolds called 'biopierces', capable of remaining in human tissue after piercing, whilst also simultaneously releasing antimicrobial drugs to prevent infection during the healing process (Figure 10D) (117). PLGA biopierces loaded with the antibiotic mupirocin showed an effective release of the drug against *S. aureus*, as confirmed by antimicrobial sensitivity testing. The zone of inhibition of the scaffolds was consistently maintained for 14 days.

SSE has also been applied to produce patches for wound-dressings applications as shown in a study where biodegradable patches with anti-microbial and wound-healing properties were developed (Figure 10E) (118). The inks used to create the patches were composed of a combination of methoxylated pectin and Manuka honey. To enhance their antimicrobial properties, inclusion complexes of propolis with beta-cyclodextrin combined with chitosan were added to the films, and *in vitro* wound-healing tests confirmed the improvement of the *in-vitro* wound-healing process. The transdermal administration of biotherapeutics through the use of microneedle patches represents an alternative to circumvent the low transdermal flux from conventional transdermal systems (127). Minimally invasive microneedle patch systems loaded with insulin were printed using alginate with different concentrations of hydroxyapatite as printing materials (Figure 10F) (78). Then, calcium chloride in solution was sprayed on the surface to crosslink the entire structure of the patches. The microneedle patches were tested in type 1 diabetic mice by the application of the patches in the dorsal skin of the animals by thumb pressing, and blood samples were collected to measure the concentration of insulin in plasma over time. The results showed that microneedles swollen and responsively released insulin in accordance with the glucose levels of the mice.

5. Other applications of SSE

5.1. 3D bioprinting

3D bioprinting involves layer by layer deposition of cell-laden biocompatible materials and supporting components to form complex and functional 3D living structures (128). At this point, it is worth mentioning the proposed difference between 'bioink' and 'biomaterial ink' since the meaning of both terms is often confused. Bioinks describe materials that include cells in their composition. Hydrogel and polymer formulations containing biological factors could be considered biomaterial inks, but are only considered bioinks after the incorporation of cells. Additionally, printed materials that are subsequently seeded with cells but not directly printed with cells, should not be considered bioinks (129).

Although different 3DP techniques are used in bioprinting such as inkjet printing, SLA, and laser induced forward transfer (LIFT), SSE 3DP is the most common (130). Amongst the advantages offered by SSE in bioprinting processes, its ability to extrude bioinks with high-cell densities and the possibility of depositing different types of cells within a predesigned structure can be accentuated. Moreover, this technology is relatively affordable and the instrumentation can be customised according to the bioink or the desired structure (130). The main disadvantages of applying SSE in bioprinting are that the mammalian cell viability may be compromised, due to the shear stress from the extrusion process, the lowest resolution achieved and longer deposition times compared to other techniques (131).

More recently, "time" has been integrated within 3D bioprinting as the fourth dimension, giving rise to a novel technique called four-dimensional (4D) bioprinting (76) (132) (Figure 11). In 4D bioprinting, live printed cellular constructs can evolve over time, changing their functionalities or reshaping themselves in response to certain external stimuli, such as temperature (133). Many studies have reviewed the use of SSE in bioprinting (133-136) so this review article only outlines below some of the most recent advances in this field.

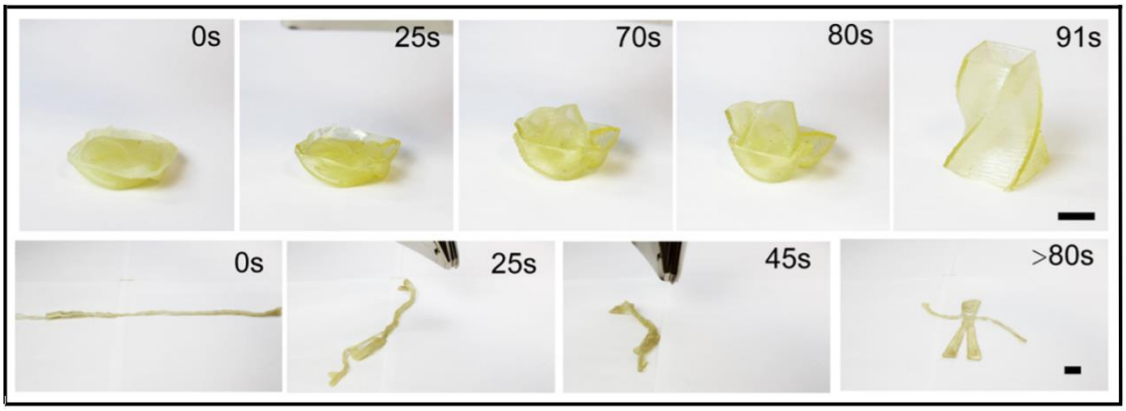

Figure 11. Photographs of 3D printed objects with shape memory properties that change from temporary shapes to permanent shapes when heated with a heat gun. Above, a compressed plate returns to its original shape as a standing hollow vase. Below, a gummy toy strand recovers to its original shape. Scale bars are 6 mm (132).

Vascularized and perfusable cardiac patches that match the anatomical and immunological characteristics of the patient have been prepared using SSE bioprinting (Figure 12A) (137). This was made possible by reprograming the patient's cells to become pluripotent stem cells and subsequently differentiate into cardiomyocytes and endothelial cells, which were later combined with hydrogels to form bioinks. These personalized patches will not elicit an immune response after transplantation since the bioinks used were originated from the same patient, thus avoiding the need for immunosuppression treatment. Moreover, it was also possible to fabricate cellularized hearts, demonstrating the potential of bioprinting to replace organs after failure (Figure 12A). However, several challenges remain to achieve this goal, such as obtaining the large number of cells necessary for engineering an organ or creating adequate blood vessel networks.

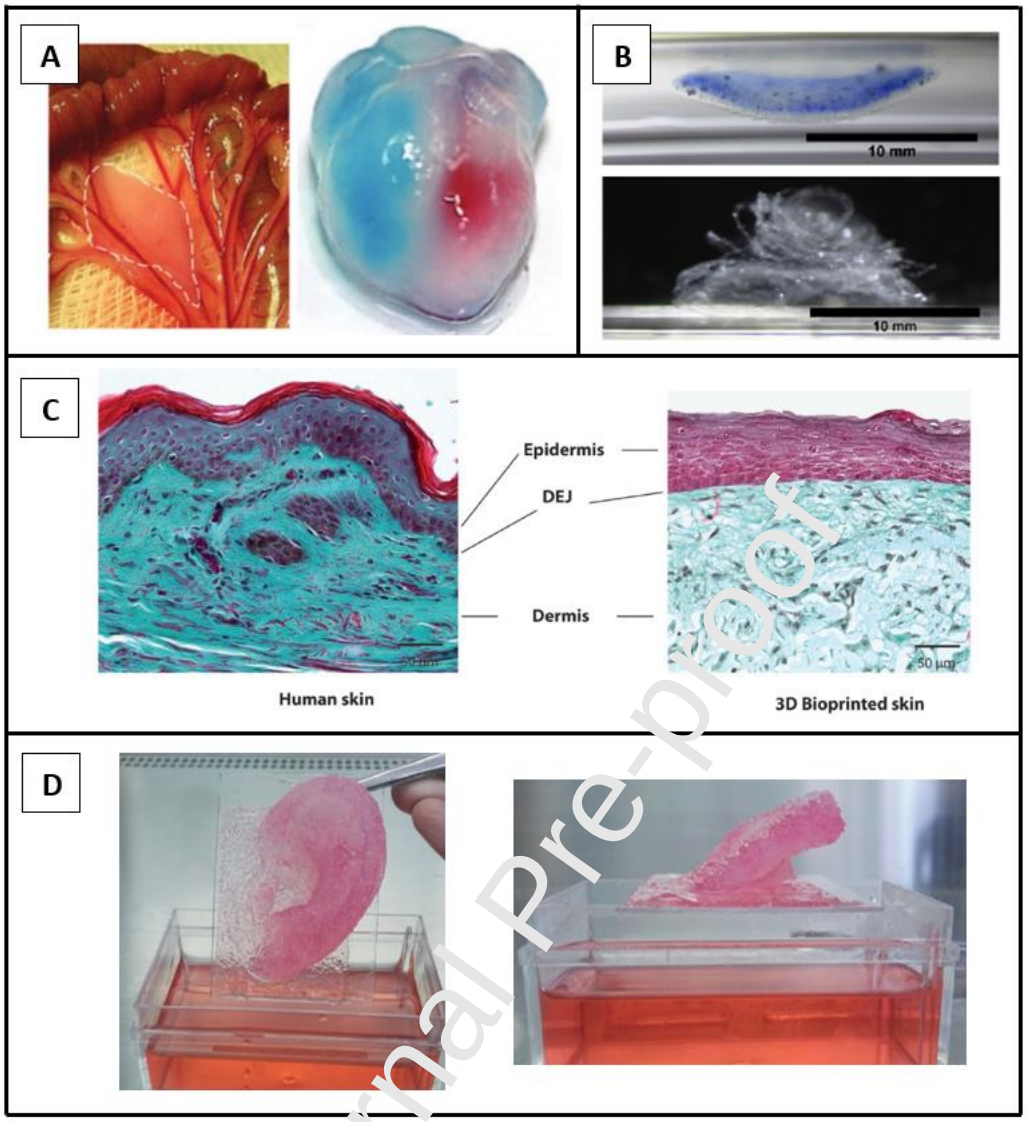

Figure 12. (A) On the left, image of a bioprinted patch transplanted in between two layers of a rat omentum. Dashed white lines delimit the edges of the patch. On the right, a bioprinted and cellularized small scale human heart with the right and left ventricles stained in blue and red, respectively (137). (B) Above, corneal structure removed from the printing support. Below, the same corneal structure beginning to unravel 1 day after printing due to the combination of keratinocytes in the bioink (138). (C) On the left, optical microscopy image of human skin and on the right, optical microscopy image of bioprinted skin after 26 days of culture (139). (D) 3D bioprinted human ear composed of human fibroblasts and bioink (139). Images reprinted and modified with permission from (137-139).

In 2018, human corneal stroma equivalents were printed for the first time using SSE bioprinting (Figure 12B) (138). The printed cornea stroma was anatomically analogous

to a human corneal model obtained from the topographic data of a human cornea. Corneal keratocytes obtained from cadaverous human corneal tissue were selected as the cell type to include in the biomaterial ink, which was composed of type I collagen and sodium alginate. High cell viability was observed even 7 days after printing, highlighting the potential of this ink for cell printing purposes. However, more research is required to analyse the corneal biocompatibility after transplantation or to improve its ability to support cell growth, among others. Furthermore, a human skin model generated with primary human skin cells was also developed using SSE. Following a scaffold-free approach, the cell-laden bioink composed of alginate, gelatin and fibrinogen was printed, generating a 5 mm thick skin (139). Significant similarities were identified between the bioprinted and human skin in the tissue cellular structuration and composition (Figure 12C). Apart from printing flat skin models, highly complex skin architectures, such as an ear, were also attempted (Figure 12D).

5.2. 3DP of electronics and bioelectronics

3DP of bioelectronics involves the production of wearable electronic devices capable of performing multi-parameter measurements and transmitting the obtained data, as well as the fabrication of biomedical devices that can mimic or enhance functionalities of biological systems (62). Bioelectronic devices are designed to be integrated into biological systems, however the degree of integration of devices produced by conventional manufacturing technologies is limited (63). 3DP enables the creation of devices using nano and microscale inks, achieving a multiscale manufacturing approach in addition to unique geometries and functionalities (140). Moreover, the printing process is often performed at room temperature which avoids harsh conditions, and the assembly of materials in three dimensions follows a bottom-up assembly process, which is in accordance with how organs and tissues are made in biological systems (141).

In this sense, some remarkable studies that have used SSE 3DP can be highlighted. For instance, by the direct extrusion of a concentrated silver nanoparticle ink it was possible to construct flexible, stretchable and extensible microelectrodes that can be patterned on a wide variety of surfaces (142). In this context, strain and pressure sensors were fabricated by employing a hybrid 3DP technique that combined SSE with an automated pick-and-place of surface mount electronic components (Figure 13A) (51). The insulating and conductive inks developed could be patterned and integrated with

electronic components of arbitrary shapes and sizes. By using SSE in combination with computer-vision-based control techniques, other researchers were capable of printing conductive inks on moving free-form surfaces (Figure 13B) (143). Specifically, both wirelessly powered devices and moisture sensors were printed on a moving human hand. Silver flakes were used as conductive fillers and added to PEO using water and ethanol as solvents. The use of ethanol increased the rate of evaporation and thus the ink drying time was reduced. In the same work, the equivalent approach was used to print living cell-laden hydrogels into the wound bed of live mice. Such developments open the possibility of directly printing wearable electronic devices on living organisms or could even be used in surgical settings. Instead of directly printing the devices on the human hand, it is also possible to extrude the ink into an elastomeric reservoir (used as a glove), as shown in a study (144) in which strain sensors were created by embedded 3DP of conducting carbon grease in the elastomeric polymer (Figure 13C).

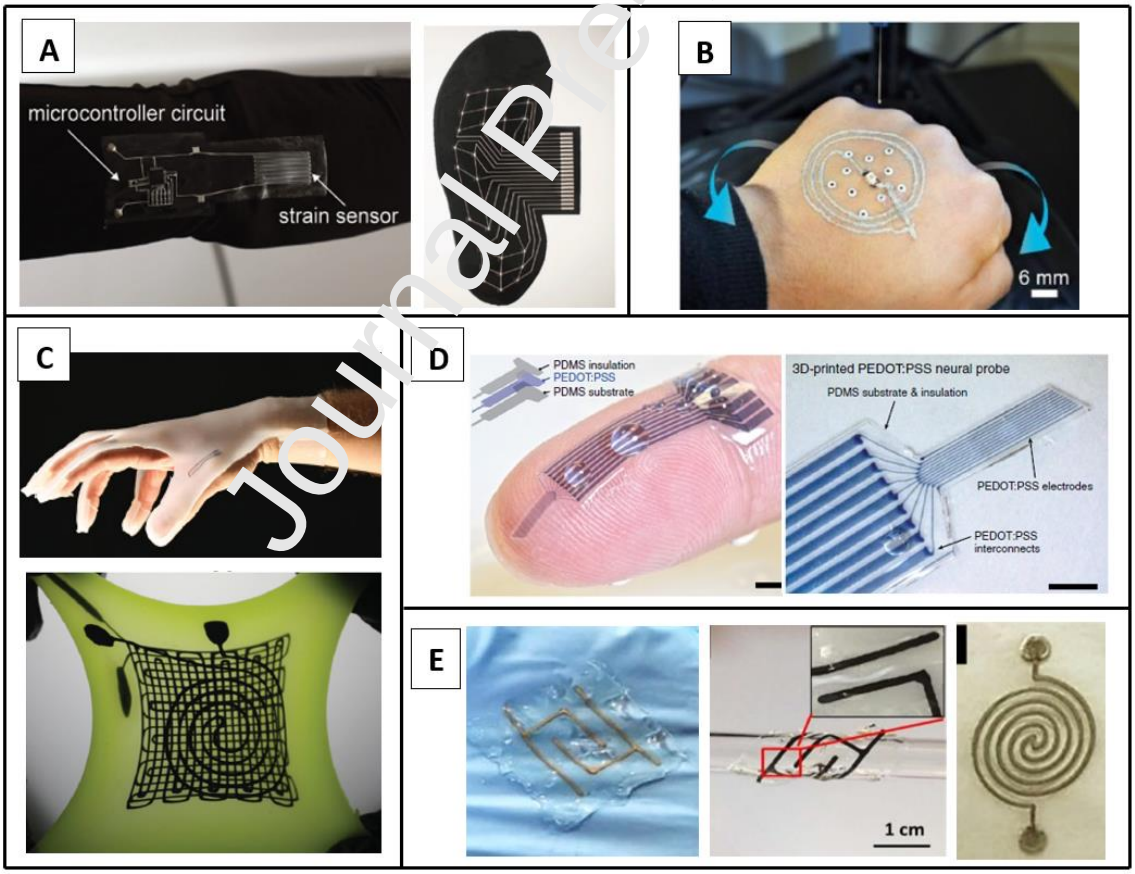

Figure 13. Images of wearable soft electronics fabricated by 3DP; (A) On the right, image of a printed textile-mounted strain sensor and microcontroller circuit and on the left, image of a plantar sensor array responsive to the application of pressure by a

human foot (51). (B) Image of a 3D printed wireless device on a human hand (freeform surface) (143). (C) Above, image of a glove with embedded strain sensors and below, a three-layer strain pressure sensor in the stretched state (144). (D) On the left, a 3D printed flexible electronic circuit made with conducting polymer ink. On the right, image of the 3D printed soft neural probe with 9-channels in magnified view (145). (E) On the left, a freestanding 3D printed platform with GelMA and silver nanoparticle ink. In the middle, conformal coverage of the same 3D printed platform showing the magnified image of the silver tracks. On the right, a 3D printed heating coil design (146). Images reproduced and modified with permission from (51, 143-146).

More recently, other conductive polymers have been developed for diverse applications, such as flexible electronics and bioelectronics. For instance, a 3D printable ink was prepared using the conducting polymers poly(3,4-ethylenedioxythiophene):polystyrene sulfonate (PEDOT:PSS) (Figure 13D) (145). The rheological behaviour of the paste-like ink was improved by the cryogenic freezing of aqueous PEDOT:PSS solution, followed by lyophilisation and subsequent redispersion in a water and dimethyl sulfoxide (DMSO) mixture. Using this ink, functional conducting polymer devices, such as a soft neural probe capable of in vivo single-unit recording, were manufactured.

In addition to creating electronics by 3D printing of conductive inks, it is also possible to deposit electronic materials on platforms manufactured by SSE 3DP. As an example, 3D platforms were fabricated using gelatin methacryloyl (GelMA) hydrogel and drop-on-demand microvalve-based printing of silver nanoparticle ink, providing the required conductivity (Figure 13E) (146). With this conductive ink, microelectrodes and heating coils were printed and embedded in the platform to be employed in various applications. Moreover, the potential of 3DP to create complex structures was exploited in another work to create electroconductive hydrogels in different forms (disc, puzzle piece design and a pentagonal arrangement of five evenly spaced cylindrical cavities) (147).

In 2013, the creation of a bionic ear using a cell-seeded hydrogel matrix along with a circular antenna made of a conducting polymer captured the attention of the media (Figure 14A) (148). Cartilage tissue was cultivated *in vitro* around the inductive coil antenna in the ear, allowing the reading of inductively coupled signals from cochlea-shaped electrodes. The ear was capable of receiving radio frequency and both the right

and left ears could listen to stereo audio. Importantly, this study demonstrated the biocompatibility of a biological structure with printed bioelectronics.

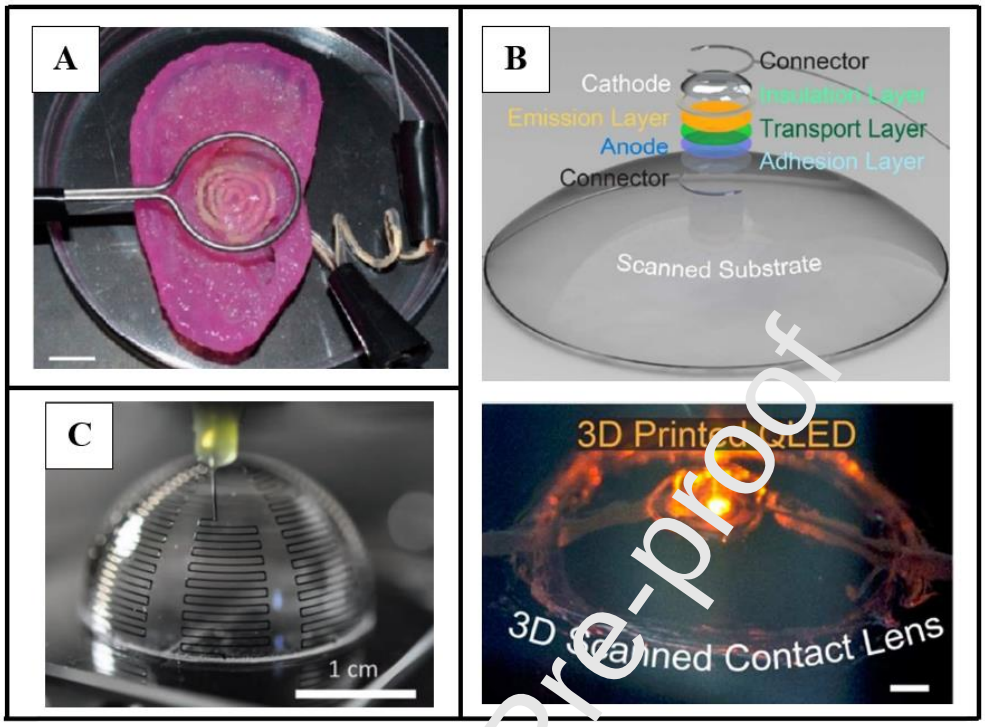

Figure 14. (A) Image of a bionic ear with a transmitting loop antenna (scale bar is 1 mm) (148). (B) On the left, CAD model showing the QD-LED components on the curvilinear surface of the contact lens. On the right, electroluminescence output from the 3D printed QD-LED (scale bar is 1 mm) (149). (C) Image of the printed electrically small antenna in the form of conductive meander lines (150). Images reproduced and modified with permission from (148-150).

Furthermore, when 3DP is coupled with 3D scanning technologies, it is possible to 3D print electronics on a 3D structure, as shown in a study in which quantum dot light-emitting diodes (QD-LED) were directly printed on the surface of contact lenses (Figure 14B) (149). A 3D light-scanning technique allowed the electronics to be tailored to the curvilinear topography of the contact lenses. The possibility of printing antennas using omnidirectional printing of silver nanoparticle inks was also reported (150). Electrically small 3D antennas were printed in the form of conductive meander lines (a series of regular sinuous curves) on curvilinear surfaces (Figure 14C). With these miniaturized antennas, a near optimal bandwidth was obtained at various frequencies, which could be of interest to create compact wireless devices for communications.

Despite significant advancements in the field of flexible 3D printed electronics and bioelectronics, many challenges need to be addressed (151). For instance, many factors such as their mechanical reliability, sensitivity, and system robustness, as well as the biocompatibility and potential toxicity of the inks used, must be carefully evaluated before implementation in real-world applications.

5.3. Food printing

The extensive amount of research using SSE in the area of food applications highlights the interest of the scientific community and the food industry towards this technology (152). As this review is focused on healthcare applications of SSE, only a few examples of food printing are mentioned. SSE is the most popular method in 3D food printing as edible materials usually are in a solid or semisolid state. For instance, it is possible to create edible chocolate-based (Figure 15A) (153) or baking dough-based (154) structures. Also, functional ingredients can be incorporated in the edible inks as shown in a study where *Bifidobacterium animalis* subsp. *Lactis BB-12* was added to mashed potatoes and printed in different forms (Figure 15B) (155). Potato starch along with celluloses and other types of starches are usually employed to improve the rheological properties of other ingredients, such as fruit juices (Figure 15C) (156). Moreover, oleogels (gels in which the continuous liquid phase is oil) can be used as inks due to their ability to incorporate liposoluble active ingredients, as shown in a study (157) where printing inks were formed using a mixture of monoglycerides (MG) and phytosterols (PS). The optimal printed dosage forms were fabricated using the mixtures with the lowest gelling temperatures, which remained partially liquid during the printing of the layers, favouring the building process.

As in the case of pharmaceutical products, SSE allows the creation of personalized foods that can be tailored according to nutritional needs, calories intake, texture, colour and flavour preferences, among others. Personalised food can be highly relevant in specific cases such as people with swallowing difficulties (e.g. the elderly), who are often provided with unappealing shredded food that affects their appetite and can lead to nutritional deficiencies. Also, people with food allergies or some conditions like diabetes could be especially benefited from this approach (61).

Figure 15. 3D food printing. (A) Chocolate-based structures (153). (B) 3D printed forms made of lemon juice and potato starch (156). (C) 3D printed structures with probiotics incorporated within potato starch (155). Images reproduced and modified with permission from (153, 155, 156).

Besides food printing, SSE can also be employed to create nanocomposites and coatings with antimicrobial properties for food packaging. One example of this application is found where gelatin films containing zinc oxide and clove essential oil were fabricated as an internal coating in packaging (158). These types of internal coatings are interesting not only for food packaging applications, but also for pharmaceutical packaging.

6. Pharmaceutical SSE 3D printers

Similarly to other 3DP technologies, SSE has evolved since the appearance of the first SSE printers. SSE 3D printers have advanced from the simplest ones that consisted of a syringe in a robotic gantry system, to printers with multiple printheads, capable of printing more than one material at the same time, with specifically designed software and higher resolution (159). An example of the technological evolution of such 3D

printers is the multi-material and multi-nozzle 3D (MM3D) printer capable of manufacturing voxelated soft matter (160). This 3D printer includes printheads capable of depositing up to eight materials that flow through separated channels until fused into a single ink before the nozzle outlet. Multiple nozzles and mechanisms that enable rapid material switching can be combined to create complex architectures composed of multiple materials that can be printed in a voxel-by-voxel manner.

Several printers have been specially designed and commercialised for bioprinting applications like 3DDiscovery (RegenHu) (161), Bioplotter (Envisiontec) (162), Regemat (163) and Bio X (Cellink) (164) to cite a few of many. These 3D printers include not only SSE, but also allow the use of other printing technologies such as FDM or inkjet printing. Some companies also provide syringes loaded with biomaterial inks, making the bioprinting process easier for the user. Conversely, to date, the only SSE 3D printer designed for pharmaceutical manufacturing is M3DIMAKER™ (FabRx) (165), although other 3D printers not designed to manufacture dosage forms are used for the same purpose. M3DIMAKER™ is specially designed for printing pharmaceutical products and includes interchangeable nozzles for the use of different 3D printing technologies, with the entire process being controlled by a validated software.

7. Regulatory aspects

As a new manufacturing technology, 3DP faces several challenges for the wide adoption in the healthcare sector, especially for highly regulated markets like the pharmaceutical industry. In 2017, the Food and Drug Administration (FDA) issued a technical guidance on medical devices and prosthetics manufactured using additive manufacturing (166). However, technical considerations and regulations concerning 3D printed products with drug delivery functions were not addressed and it is expected to be issued in the future. To date, Spritam®, by Aprecia Pharmaceuticals (167) is the only 3D printed drug product approved for commercialisation. Unlike the case of Spritam®, which uses a technology adapted to large-scale manufacture, the on-demand production of medicines through 3D printing does not fall under the same regulations and therefore its implementation requires new regulatory agreements.

Another key aspect for the implementation of 3DP in healthcare is the standardization of 3D printers to meet regulatory and quality control (QC) requirements, as well as the

use of a validated software to control the entire process. Moreover, whether on an industrial scale or applied to the on-demand manufacture of drug products, it is convenient to use Process Analytical Technology (PAT) to ensure greater process performance and product quality (168). Several studies have proposed non-destructive in-line analytical techniques for real time quality control measurements. As an example of PAT tools, spectroscopic techniques such as near infrared (NIR) and Raman spectroscopy have been shown to be capable of performing quality control measures in a non-destructive manner (169, 170). The inclusion of QR codes and data matrices on dosage forms as track-and-trace measures to ensure product quality and safety were also suggested (171, 172).

On the other hand, although different 3D printers were used to print dosage forms and medical devices in the research field, those 3D printers were not adapted for the production of pharmaceutical products and hence do not meet the Good Manufacturing Practise (GMP) regulations (168). To date, there is only one commercially available 3D printer that has been especially designed for the manufacture of personalised medicines, which can be fully validated according to GMP regulations (165). Furthermore, certain 3DP technologies are more suitable than others for personalised medicine production. SSE, for example, has the potential to be one of the first technologies to be employed for the production of medicines as most of the excipients used to prepare the formulations are either pharmaceutical or food-grade excipients or are listed as GRAS (Generally Recognized As Safe) (173). Conversely, other technologies such as vat photopolymerisation techniques, use materials with potential *in vivo* toxicity or which may undergo unexpected chemical reactions with the drug (174). As such, some safety issues and regulatory gaps still need to be addressed prior to the implementation of these technologies in healthcare.

8. Advantages and limitations of SSE 3DP

SSE is perhaps the most suitable technology for producing personalized medicines, alongside other 3DP technologies such as FDM and DPE due to the wide array of dosage forms that can be formulated (ODFs, chewable printlets, polypills, etc.) in a variety of shapes and flavours (20, 24, 59, 75). The main advantage of this technology lies in its simplicity, since the drug can be directly mixed with the excipients and filled into a syringe or cartridge for printing (38). Alternatively, the use of disposable syringes

in a similar fashion to how coffee capsules are used in coffee machines helps maintain a clean environment and facilitates GMP compliance (175). In an ideal scenario, the physician would make an individualised digital prescription for the patient, followed by the preparation of a tailored and personalised formulation. The materials, mixture of excipients and drug, to prepare the formulations or 'ink' could be i) fabricated in an industrial facility by a pharmaceutical company in a similar fashion to commercial coffee pods or ii) prepared in the pharmacy in a similar fashion to traditional coffee making.

Printlets with the exact dose can be printed directly into the blister packing, saving time and reducing the risk of contamination and dosing errors as a result of manual compounding. Moreover, SSE is particularly amenable for producing patient-friendly formulations to aid medication adherence, as it is possible to create chewable formulations for patients with swallowing difficulties like geriatrics. Children's preferences towards chewable dosage forms is also well known, and this technology could facilitate the creation of appropriate medicines to meet the needs and preferences of these patients (60).

Besides its potential clinical applications, SSE is also beneficial for formulating drugs to be used in preclinical studies. In a preclinical setting, SSE enables the production of devices and dosage forms tailored to the study requirements, overcoming the problems arising from the lack of specially designed equipment to prepare formulations for animal testing (176). In addition to oral dosage forms adapted in size and dose for administration to animals, this technology could be employed to produce dosage forms typically formulated using soft materials, such as rectal forms (20). Moreover, as the materials are solids that possess a relatively low melting point or are in a semisolid state at room temperature, the use of high temperatures is avoided and thus drug degradation is prevented. The low temperatures required during the printing process allow the manufacture of implants and patches loaded with live cells, as well as proteins or other thermosensitive drugs (97, 137).

While the advantages of SSE are evident, there are some issues that must be considered to achieve an optimal printing process. The viscosity of the materials can be easily modified by manipulating the temperature, pH, or excipient amount to obtain a printable

feedstock. However, these modifications could lead to changes in the physical state of the drug and require further optimisation (38). The necessary drying time can vary from one formulation to another, depending on the materials being used. Although some formulations harden a few minutes after printing, others need a post-printing drying process to ensure the correct solidification of the printlet (98). If there are solvents involved in the preparation of the feedstock material, a final solvent evaporation step is necessary to ensure complete solvent removal. Moreover, the viscosity of the materials is directly linked to the requirement for a drying step. Less viscous feedstocks generally require more drying time and are also associated with an increased risk of material collapse and loss of shape (107).

In terms of printing speed and resolution, the speed rate obtained with SSE is higher compared to other technologies, which is a clear advantage in view of its future implementation in clinical practice. However, the resolution at which SSE printers are capable of printing is often low (122). The resolution can be improved by using nozzles with narrower orifices, but this does not always work for highly viscous materials that require wider nozzle diameters. Although a lower resolution may affect the accuracy with which the printlets are developed, this, on the other hand, allows achieving the faster printing speed mentioned above.

Apart from the limitations mentioned above, before these tailor-made dosage forms can be implemented in healthcare, there are still some aspects to explore, such as how prolonged storage could affect the properties of the printing materials (95). Although the printlets could be manufactured immediately before administration and therefore long-term stability studies would not be necessary, it might also be beneficial to store pre-filled syringes with the formulation ready to be printed when needed. An ideal formulation could be stored for on demand production of printlet batches at the point of care, for example in hospital settings, saving time and reducing costs that would otherwise be used to prepare new formulations each time a compounded formulation is required.

9. Conclusions

SSE 3DP has the potential to revolutionise healthcare and medicines manufacture. This versatile technology that employs semisolid or semi-molten materials can create

complex structures with personalised characteristics. SSE enables the preparation of medicines with different geometries and release profiles that can also be tailored to individual patient preferences in terms of flavour profiles and colours. Moreover, the use of disposable syringes facilitates the entire process, helping to meet strict quality control requirements. Also applied in bioprinting applications, the low temperatures required for material extrusion make this technique suitable for printing cell-laden tissues such as skin tissue, corneas, and cardiac patches, among others. More recently, this technology has shown its potential in the field of bioelectronics, particularly in the production of biosensors capable of monitoring physiological parameters of the human body. All these achievements are paving the way for a more personalized treatment approach, from more accurate diagnosis to patient tailored medicines.

Acknowledgements

This research was funded by the Engineering and Physical Sciences Research Council (EPSRC) UK grant number EP/S023054/1 and by Xunta de Galicia grant number GRC2013/015 and GPC2017/015.

REFERENCES

1. Durga Prasad Reddy R, Sharma V. Additive manufacturing in drug delivery applications: A review. International Journal of Pharmaceutics. 2020;589:119820.

2. Capel AJ, Rimington RP, Lewis MP, Christie SDR. 3D printing for chemical, pharmaceutical and biological applications. Nature Reviews Chemistry. 2018;2(12):422-36.

3. Chen G, Xu Y, Chi Lip Kwok P, Kang L. Pharmaceutical Applications of 3D Printing. Additive Manufacturing. 2020;34:101209.

4. ASTM. Standard Terminology for Additive Manufacturing Technologies. F2792 − 12a. 2012.

5. Infanger S, Haemmerli A, Iliev S, Baier A, Stoyanov E, Quodbach J. Powder bed 3D-printing of highly loaded drug delivery devices with hydroxypropyl cellulose as solid binder. Int J Pharm. 2019;555:198-206.

6. Shi K, Tan DK, Nokhodchi A, Maniruzzaman M. Drop-On-Powder 3D Printing of Tablets with an Anti-Cancer Drug, 5-Fluorouracil. Pharmaceutics. 2019;11(4).

7. Boudriau S, Hanzel C, Massicotte J, Savegh L, Wang J, Lefebvre M. Randomized Comparative Bioavailability of a Novel Three-Dimensional Printed Fast-Melt Formulation of Levetiracetam Following the Administration of a Single 1000-mg Dose to Healthy Human Volunteers Under Fasting and Fed Conditions. Drugs R D. 2016;16(2):229-38.

8. Sen K, Mukherjee R, Sansare S, Halder A, Kashi H, Ma AWK, et al. Impact of powder-binder interactions on 3D printability of pharmaceutical tablets using drop test methodology. European Journal of Pharmaceutical Sciences. 2021:105755.

9. Goyanes A, Buanz AB, Basit AW, Gaisford S. Fused-filament 3D printing (3DP) for fabrication of tablets. Int J Pharm. 2014;476(1-2):88-92.

10. Elbadawi M, Muñiz Castro B, Gavins FKH, Jie Ong J, Gaisford S, Pérez G, et al. M3DISEEN: A Novel Machine Learning Approach for Predicting the 3D Printability of Medicines. Int J Pharm. 2020:119837.

11. Tiboni M, Campana R, Frangipani E, Casettari L. 3D printed clotrimazole intravaginal ring for the treatment of recurrent vaginal candidiasis. International Journal of Pharmaceutics. 2021;596:120290.

12. Ghanizadeh Tabriz A, Nandi U, Hurt AP, Hui H-W, Karki S, Gong Y, et al. 3D printed bilayer tablet with dual controlled drug release for tuberculosis treatment. International Journal of Pharmaceutics. 2021;593:120147.

13. Öblom H, Cornett C, Bøtker J, Frokjaer S, Hansen H, Rades T, et al. Data-enriched edible pharmaceuticals (DEEP) of medical cannabis by inkjet printing. International Journal of Pharmaceutics. 2020;589:119866.

14. Dodoo CC, Stapleton P, Basit AW, Gaisford S. The potential of Streptococcus salivarius oral films in the management of dental caries: An inkjet printing approach. International Journal of Pharmaceutics. 2020;591:119962.

15. Kyobula M, Adedeji A, Alexander MR, Saleh E, Wildman R, Ashcroft I, et al. 3D inkjet printing of tablets exploiting bespoke complex geometries for controlled and tuneable drug release. Journal of Controlled Release. 2017;261:207-15.

16. Clark EA, Alexander MR, Irvine DJ, Roberts CJ, Wallace MJ, Sharpe S, et al. 3D printing of tablets using inkjet with UV photoinitiation. International Journal of Pharmaceutics. 2017;529(1):523-30.

17. Goyanes A, Allahham N, Trenfield SJ, Stoyanov E, Gaisford S, Basit AW. Direct powder extrusion 3D printing: Fabrication of drug products using a novel single-step process. Int J Pharm. 2019;567:118471.

18. Ong JJ, Awad A, Martorana A, Gaisford S, Stoyanov E, Basit AW, et al. 3D printed opioid medicines with alcohol-resistant and abuse-deterrent properties. Int J Pharm. 2020;579:119169.

19. Fanous M, Gold S, Muller S, Hirsch S, Ogorka J, Imanidis G. Simplification of fused deposition modeling 3D-printing paradigm: Feasibility of 1-step direct powder printing for immediate release dosage form production. International Journal of Pharmaceutics. 2020;578:119124.

20. Seoane-Viaño I, Ong JJ, Luzardo-Alvarez A, González-Barcia M, Basit AW, Otero-Espinar FJ, et al. 3D printed tacrolimus suppositories for the treatment of ulcerative colitis. Asian Journal of Pharmaceutical Sciences. 2020.

21. Fang D, Yang Y, Cui M, Pan H, Wang L, Li P, et al. Three-Dimensional (3D)–Printed Zero-Order Released Platform: a Novel Method of Personalized Dosage Form Design and Manufacturing. AAPS PharmSciTech. 2021;22(1):37.

22. Seoane-Viaño I, Gómez-Lado N, Lázare-Iglesias H, García-Otero X, Antúnez-López JR, Ruibal Á, et al. 3D Printed Tacrolimus Rectal Formulations Ameliorate Colitis in an Experimental Animal Model of Inflammatory Bowel Disease. Biomedicines. 2020;8(12).

23. Tagami T, Ito E, Kida R, Hirose K, Noda T, Ozeki T. 3D printing of gummy drug formulations composed of gelatin and an HPMC-based hydrogel for pediatric use. International Journal of Pharmaceutics. 2021;594:120118.

24. Yan TT, Lv ZF, Tian P, Lin MM, Lin W, Huang SY, et al. Semi-solid extrusion 3D printing ODFs: an individual drug delivery system for small scale pharmacy. Drug Dev Ind Pharm. 2020;46(4):531-8.

25. Hamed R, Mohamed EM, Rahman Z, Khan MA. 3D-printing of lopinavir printlets by selective laser sintering and quantification of crystalline fraction by XRPD-chemometric models. International Journal of Pharmaceutics. 2021;592:120059.

26. Yang Y, Xu Y, Wei S, Shan W. Oral preparations with tunable dissolution behavior based on selective laser sintering technique. International Journal of Pharmaceutics. 2021;593:120127.

27. Allahham N, Fina F, Marcuta C, Kraschew L, Mohr W, Gaisford S, et al. Selective Laser Sintering 3D Printing of Orally Disintegrating Printlets Containing Ondansetron. Pharmaceutics. 2020;12(2).

28. Mohamed EM, Barakh Ali SF, Rahman Z, Dharani S, Ozkan T, Kuttolamadom MA, et al. Formulation Optimization of Selective Laser Sintering 3D-Printed Tablets of Clindamycin Palmitate Hydrochloride by Response Surface Methodology. AAPS PharmSciTech. 2020;21(6):232.

29. Gueche YA, Sanchez-Ballester NM, Bataille B, Aubert A, Leclercq L, Rossi J-C, et al. Selective Laser Sintering of Solid Oral Dosage Forms with Copovidone and Paracetamol Using a CO2 Laser. Pharmaceutics. 2021;13(7).

30. Xu X, Awad A, Martinez PR, Gaisford S, Goyanes A, Basit AW. Vat photopolymerization 3D printing for advanced drug delivery and medical device applications. Journal of Controlled Release. 2020.

31. Li W, Mille LS, Robledo JA, Uribe T, Huerta V, Zhang YS. Recent Advances in Formulating and Processing Biomaterial Inks for Vat Polymerization-Based 3D Printing. Advanced Healthcare Materials. 2020;9(15):2000156.

32. Xu X, Goyanes A, Trenfield SJ, Diaz-Gomez L, Alvarez-Lorenzo C, Gaisford S, et al. Stereolithography (SLA) 3D printing of a bladder device for intravesical drug delivery. Materials Science and Engineering: C. 2021;120:111773.

33. Wilts EM, Gula A, Davis C, Chartrain N, Williams CB, Long TE. Vat photopolymerization of liquid, biodegradable PLGA-based oligomers as tissue scaffolds. European Polymer Journal. 2020;130:109693.

34. Norman J, Madurawe RD, Moore CMV, Khan MA, Khairuzzaman A. A new chapter in pharmaceutical manufacturing: 3D-printed drug products. Adv Drug Deliv Rev. 2017;108:39-50.

35. Ayyoubi S, Cerda JR, Fernández-García R, Knief P, Lalatsa A, Marie Healy A, et al. 3D printed spherical mini-tablets: Geometry versus composition effects in controlling dissolution from personalised solid dosage forms. International Journal of Pharmaceutics. 2021:120336.

36. Zhang J, Thakkar R, Zhang Y, Maniruzzaman M. Structure-function correlation and personalized 3D printed tablets using a quality by design (QbD) approach. International Journal of Pharmaceutics. 2020;590:119945.

37. Jie Neriah Tan Y, Pong Yong W, Low H, Singh Kochhar J, Khanolkar J, Teng Shuen Ernest L, et al. Customizable Drug Tablets with Constant Release Profiles via 3D Printing Technology. International Journal of Pharmaceutics. 2021:120370.

38. Firth J, Basit AW, Gaisford S. The Role of Semi-Solid Extrusion Printing in Clinical Practice. In: Basit AW, Gaisford S, editors. 3D Printing of Pharmaceuticals: Springer International Publishing; 2018. p. 133-51.

39. Shi K, Slavage JP, Maniruzzaman M, Nokhodchi A. Role of release modifiers to modulate drug release from fused deposition modelling (FDM) 3D printed tablets. International Journal of Pharmaceutics. 2021;597:120315.

40. Samaro A, Janssens P, Vanhoorne V, Van Renterghem J, Eeckhout M, Cardon L, et al. Screening of pharmaceutical polymers for extrusion-Based Additive Manufacturing of patient-tailored tablets. International Journal of Pharmaceutics. 2020;586:119591.

41. Henry S, Samaro A, Marchesini FH, Shaqour B, Macedo J, Vanhoorne V, et al. Extrusion-based 3D printing of oral solid dosage forms: material requirements and equipment dependencies. International Journal of Pharmaceutics. 2021:120361.

42. Liaskoni A, Wildman RD, Roberts CJ. 3D printed polymeric drug-eluting implants. International Journal of Pharmaceutics. 2021;597:120330.

43. El Aita I, Breitkreutz J, Quodbach J. On-demand manufacturing of immediate release levetiracetam tablets using pressure-assisted microsyringe printing. Eur J Pharm Biopharm. 2019;134:29-36.

44. El Aita I, Rahman J, Breitkreutz J, Quodbach J. 3D-Printing with precise layer-wise dose adjustments for paediatric use via pressure-assisted microsyringe printing. Eur J Pharm Biopharm. 2020;157:59-65.

45. Aguilar-de-Leyva Á, Linares V, Casas M, Caraballo I. 3D Printed Drug Delivery Systems Based on Natural Products. Pharmaceutics. 2020;12(7).

46. Feilden E, Blanca EG-T, Giuliani F, Saiz E, Vandeperre L. Robocasting of structural ceramic parts with hydrogel inks. Journal of the European Ceramic Society. 2016;36(10):2525-33.

47. Gholamipour-Shirazi A, Norton IT, Mills T. Designing hydrocolloid based food-ink formulations for extrusion 3D printing. Food Hydrocolloids. 2019;95:161-7.

48. Godoi FC, Prakash S, Bhandari BR. 3d printing technologies applied for food design: Status and prospects. Journal of Food Engineering. 2016;179:44-54.

49. Li P, Jia H, Zhang S, Yang Y, Sun H, Wang H, et al. Thermal Extrusion 3D Printing for the Fabrication of Puerarin Immediate-Release Tablets. AAPS PharmSciTech. 2019;21(1):20.

50. Pablo Real J, Eugenia Barberis M, Camacho NM, Sánchez Bruni S, Palma SD. Design of Novel oral Ricobendazole Formulation applying Melting solidification printing process (MESO-PP): An Innovative Solvent-Free Alternative Method for 3D Printing Using a Simplified Concept and Low temperature. Int J Pharm. 2020:119653.

51. Valentine AD, Busbee TA, Boley JW, Raney JR, Chortos A, Kotikian A, et al. Hybrid 3D Printing of Soft Electronics. Advanced Materials. 2017;29(40):1703817.

52. Musazzi UM, Selmin F, Ortenzi MA, Mohammed GK, Franzé S, Minghetti P, et al. Personalized orodispersible films by hot melt ram extrusion 3D printing. Int J Pharm. 2018;551(1):52-9.

53. Cho HW, Baek SH, Lee BJ, Jin HE. Orodispersible Polymer Films with the Poorly Water-Soluble Drug, Olanzapine: Hot-Melt Pneumatic Extrusion for Single-Process 3D Printing. Pharmaceutics. 2020;12(8).

54. Ozbolat IT, Hospodiuk M. Current advances and future perspectives in extrusion-based bioprinting. Biomaterials. 2016;76:321-43.

55. Hospodiuk M, Moncal KK, Dey M, Ozbolat IT. Extrusion-Based Biofabrication in Tissue Engineering and Regenerative Medicine. In: Ovsianikov A, Yoo J, Mironov V, editors. 3D Printing and Biofabrication. Cham: Springer International Publishing; 2018. p. 255-81.

56. Duan B, Kapetanovic E, Hockaday LA, Butcher JT. Three-dimensional printed trileaflet valve conduits using biological hydrogels and human valve interstitial cells. Acta Biomater. 2014;10(5):1836-46.

57. Cui X, Breitenkamp K, Finn MG, Lotz M, D'Lima DD. Direct Human Cartilage Repair Using Three-Dimensional Bioprinting Technology. Tissue Engineering Part A. 2012;18(11-12):1304-12.

58. Park BJ, Choi HJ, Moon SJ, Kim SJ, Bajracharya R, Min JY, et al. Pharmaceutical applications of 3D printing technology: current understanding and future perspectives. Journal of Pharmaceutical Investigation. 2019;49(6):575-85.

59. Goyanes A, Madla CM, Umaji A, Duran Piñeiro G, Giraldez Montero JM, Lamas Diaz MJ, et al. Automated therapy preparation of isoleucine formulations using 3D printing for the treatment of MSUD: First single-centre, prospective, crossover study in patients. International Journal of Pharmaceutics. 2019;567:118497.

60. Januskaite P, Xu X, Ranmal SR, Gaisford S, Basit AW, Tuleu C, et al. I Spy with My Little Eye: A Paediatric Visual Preferences Survey of 3D Printed Tablets. Pharmaceutics. 2020;12(11).

61. Le-Bail A, Maniglia BC, Le-Bail P. Recent advances and future perspective in additive manufacturing of foods based on 3D printing. Current Opinion in Food Science. 2020;35:54-64.

62. Hwang HH, Zhu W, Victorine G, Lawrence N, Chen S. 3D-Printing of Functional Biomedical Microdevices via Light- and Extrusion-Based Approaches. Small Methods. 2018;2(2).

63. Ghosh U, Ning S, Wang Y, Kong YL. Addressing Unmet Clinical Needs with 3D Printing Technologies. Advanced Healthcare Materials. 2018;7(17):1800417.

64. Trenfield S, Madla C, Basit A, Gaisford S. The Shape of Things to Come: Emerging Applications of 3D Printing in Healthcare. 2018. p. 1-19.

65. Ozbolat IT. 3D Bioprinting: Fundamentals, Principles and Applications2016. 1-342 p.

66. Tagami T, Ando M, Nagata N, Goto E, Yoshimura N, Takeuchi T, et al. Fabrication of Naftopidil-Loaded Tablets Using a Semisolid Extrusion-Type 3D Printer and the Characteristics of the Printed Hydrogel and Resulting Tablets. Journal of Pharmaceutical Sciences. 2019;108(2):907-13.

67. Zidan A, Alayoubi A, Coburn J, Asfari S, Ghammraoui B, Cruz CN, et al. Extrudability analysis of drug loaded pastes for 3D printing of modified release tablets. International Journal of Pharmaceutics. 2019;554:292-301.

68. Liu Z, Zhang M. Chapter 2 - 3D Food Printing Technologies and Factors Affecting Printing Precision. In: Godoi FC, Bhandari BR, Prakash S, Zhang M, editors. Fundamentals of 3D Food Printing and Applications: Academic Press; 2019. p. 19-40.

69. Zhu S, Stieger MA, van der Goot AJ, Schutyser MAI. Extrusion-based 3D printing of food pastes: Correlating rheological properties with printing behaviour. Innovative Food Science & Emerging Technologies. 2019;58:102214.

70. Khalil S, Sun W. Biopolymer deposition for freeform fabrication of hydrogel tissue constructs. Materials Science and Engineering: C. 2007;27(3):469-78.

71. Vithani K, Goyanes A, Jannin V, Basit AW, Gaisford S, Boyd BJ. A Proof of Concept for 3D Printing of Solid Lipid-Based Formulations of Poorly Water-Soluble Drugs to Control Formulation Dispersion Kinetics. Pharmaceutical Research. 2019;36(7):102.

72. Gibson I, Rosen DW, Stucker B. Extrusion-Based Systems. In: Gibson I, Rosen DW, Stucker B, editors. Additive Manufacturing Technologies: Rapid Prototyping to Direct Digital Manufacturing. Boston, MA: Springer US; 2010. p. 160-86.

73. Hsiang Loh G, Pei E, Gonzalez-Gutierrez J, Monzón M. An Overview of Material Extrusion Troubleshooting. Applied Sciences. 2020;10(14).

74. Singh K. Experimental study to prevent the warping of 3D models in fused deposition modeling. International Journal of Plastics Technology. 2018;22(1):177-84.

75. Khaled SA, Burley JC, Alexander MR, Yang J, Roberts CJ. 3D printing of five-in-one dose combination polypill with defined immediate and sustained release profiles. J Control Release. 2015;217:308-14.

76. Sydney Gladman A, Matsumoto EA, Nuzzo RG, Mahadevan L, Lewis JA. Biomimetic 4D printing. Nat Mater. 2016;advance online publication.

77. Holländer J, Hakala R, Suominen J, Moritz N, Yliruusi J, Sandler N. 3D printed UV light cured polydimethylsiloxane devices for drug delivery. International Journal of Pharmaceutics. 2018;544(2):433-42.

78. Wu M, Zhang Y, Huang H, Li J, Liu H, Guo Z, et al. Assisted 3D printing of microneedle patches for minimally invasive glucose control in diabetes. Materials Science and Engineering: C. 2020;117:111299.

79. Croitoru-Sadger T, Yogev S, Shabtay-Orbach A, Mizrahi B. Two-component cross-linkable gels for fabrication of solid oral dosage forms. Journal of Controlled Release. 2019;303:274-80.

80. Azad MA, Olawuni D, Kimbell G, Badruddoza AZM, Hossain MS, Sultana T. Polymers for Extrusion-Based 3D Printing of Pharmaceuticals: A Holistic Materials-Process Perspective. Pharmaceutics. 2020;12(2).

81. Oliveira SM, Fasolin LH, Vicente AA, Fuciños P, Pastrana LM. Printability, microstructure, and flow dynamics of phase-separated edible 3D inks. Food Hydrocolloids. 2020;109:106120.

82. Zidan A, Alayoubi A, Asfari S, Coburn J, Ghammraoui B, Aqueel S, et al. Development of mechanistic models to identify critical formulation and process variables of pastes for 3D printing of modified release tablets. Int J Pharm. 2019;555:109-23.

83. Jiang Y, Zhou J, Feng C, Shi H, Zhao G, Bian Y. Rheological behavior, 3D printability and the formation of scaffolds with cellulose nanocrystals/gelatin hydrogels. Journal of Materials Science. 2020;55(33):15709-25.

84. Goyanes A, Fina F, Martorana A, Sedough D, Caisford S, Basit AW. Development of modified release 3D printed tablets (printlets) with pharmaceutical excipients using additive manufacturing. International Journal of Pharmaceutics. 2017;527(1–2):21-30.

85. Duty C, Ajinjeru C, Kishore V, Compton B, Hmeidat N, Chen X, et al. What makes a material printable? A viscoelastic model for extrusion-based 3D printing of polymers. Journal of Manufacturing Processes. 2018;35:526-37.

86. Oyinloye TM, Yoon WB. Stability of 3D printing using a mixture of pea protein and alginate: Precision and application of additive layer manufacturing simulation approach for stress distribution. Journal of Food Engineering. 2021;288:110127.

87. Moeini MA, Hosseinpoor M, Yahia A. Effectiveness of the rheometric methods to evaluate the buildup of cementitious mortars used for 3D printing. Construction and Building Materials. 2020;257:119551.

88. Liu Z, Zhang M, Ye Y. Indirect prediction of 3D printability of mashed potatoes based on LF-NMR measurements. Journal of Food Engineering. 2020;287:110137.

89. Conceição J, Farto-Vaamonde X, Goyanes A, Adeoye O, Concheiro A, Cabral-Marques H, et al. Hydroxypropyl-β-cyclodextrin-based fast dissolving carbamazepine printlets prepared by semisolid extrusion 3D printing. Carbohydr Polym. 2019;221:55-62.

90. García-Tuñón E, Feilden E, Zheng H, D'Elia E, Leong A, Saiz E. Graphene Oxide: An All-in-One Processing Additive for 3D Printing. ACS Applied Materials & Interfaces. 2017;9(38):32977-89.

91. Michel R, Auzély-Velty R. Hydrogel-Colloid Composite Bioinks for Targeted Tissue-Printing. Biomacromolecules. 2020;21(8):2949-65.

92. Álvarez-Castillo E, Oliveira S, Bengoechea C, Sousa I, Raymundo A, Guerrero A. A rheological approach to 3D printing of plasma protein based doughs. Journal of Food Engineering. 2021;288:110255.

93. Herrada-Manchón H, Rodríguez-González D, Alejandro Fernández M, Suñé-Pou M, Pérez-Lozano P, García-Montoya E, et al. 3D printed gummies: Personalized drug dosage in a safe and appealing way. International Journal of Pharmaceutics. 2020;587:119687.

94. Goyanes A, Buanz AB, Hatton GB, Gaisford S, Basit AW. 3D printing of modified-release aminosalicylate (4-ASA and 5-ASA) tablets. Eur J Pharm Biopharm. 2015;89:157-62.

95. Aita IE, Breitkreutz J, Quodbach J. Investigation of semi-solid formulations for 3D printing of drugs after prolonged storage to mimic real-life applications. Eur J Pharm Sci. 2020;146:105266.

96. Elbl J, Gajdziok J, Kolarczyk J. 3D printing of multilayered orodispersible films with in-process drying. International Journal of Pharmaceutics. 2020;575:118883.

97. Yi HG, Choi YJ, Kang KS, Hong JM, Pati RG, Park MN, et al. A 3D-printed local drug delivery patch for pancreatic cancer growth suppression. J Control Release. 2016;238:231-41.

98. Khaled SA, Burley JC, Alexander MR, Yang J, Roberts CJ. 3D printing of tablets containing multiple drugs with defined release profiles. Int J Pharm. 2015;494(2):643-50.

99. Haring AP, Tong Y, Halper J, Johnson BN. Programming of Multicomponent Temporal Release Profiles in 3D Printed Polypills via Core–Shell, Multilayer, and Gradient Concentration Profiles. Advanced Healthcare Materials. 2018;7(16):1800213.

100. Siyawamwaya M, du Toit LC, Kumar P, Choonara YE, Kondiah PPPD, Pillay V. 3D printed, controlled release, tritherapeutic tablet matrix for advanced anti-HIV-1 drug delivery. European Journal of Pharmaceutics and Biopharmaceutics. 2019;138:99-110.

101. Zheng Z, Lv J, Yang W, Pi X, Lin W, Lin Z, et al. Preparation and application of subdivided tablets using 3D printing for precise hospital dispensing. European Journal of Pharmaceutical Sciences. 2020;149:105293.

102. Khaled SA, Alexander MR, Wildman RD, Wallace MJ, Sharpe S, Yoo J, et al. 3D extrusion printing of high drug loading immediate release paracetamol tablets. Int J Pharm. 2018;538(1–2):223-30.

103. Cui M, Pan H, Fang D, Qiao S, Wang S, Pan W. Fabrication of high drug loading levetiracetam tablets using semi-solid extrusion 3D printing. Journal of Drug Delivery Science and Technology. 2020;57:101683.

104. Cui M, Li Y, Wang S, Chai Y, Lou J, Chen F, et al. Exploration and Preparation of a Dose-Flexible Regulation System for Levetiracetam Tablets via Novel Semi-Solid Extrusion Three-Dimensional Printing. J Pharm Sci. 2019;108(2):977-86.

105. Yang Y, Wang X, Lin X, Xie L, Ivone R, Shen J, et al. A tunable extruded 3D printing platform using thermo-sensitive pastes. International Journal of Pharmaceutics. 2020;583:119360.

106. Khaled SA, Burley JC, Alexander MR, Roberts CJ. Desktop 3D printing of controlled release pharmaceutical bilayer tablets. Int J Pharm. 2014;461(1-2):105-11.

107. Cheng Y, Qin H, Acevedo NC, Jiang X, Shi X. 3D printing of extended-release tablets of theophylline using hydroxypropyl methylcellulose (HPMC) hydrogels. Int J Pharm. 2020;591:119983.

108. Cui M, Yang Y, Jia D, Li P, Li Q, Chen F, et al. Effect of novel internal structures on printability and drug release behavior of 3D printed tablets. Journal of Drug Delivery Science and Technology. 2019;49:14-23.

109. Li Q, Guan X, Cui M, Zhu Z, Chen K, Wen H, et al. Preparation and investigation of novel gastro-floating tablets with 3D extrusion-based printing. Int J Pharm. 2018;535(1):325-32.

110. Karavasili C, Gkaragkounis A, Moschakis T, Ritzoulis C, Fatouros DG. Pediatric-friendly chocolate-based dosage forms for the oral administration of both hydrophilic and lipophilic drugs fabricated with extrusion-based 3D printing. European Journal of Pharmaceutical Sciences. 2020;147:105291.

111. Rycerz K, Stepien KA, Czapiewska M, Arafat BT, Habashy R, Isreb A, et al. Embedded 3D Printing of Novel Bespoke Soft Dosage Form Concept for Pediatrics. Pharmaceutics. 2019;11(12).

112. Sjöholm E, Sandler N. Additive manufacturing of personalized orodispersible warfarin films. International Journal of Pharmaceutics. 2019;564:117-23.

113. Oblom H, Sjoholm E, Rautamo M, Sandler N. Towards Printed Pediatric Medicines in Hospital Pharmacies: Comparison of 2D and 3D-Printed Orodispersible Warfarin Films with Conventional Oral Powders in Unit Dose Sachets. Pharmaceutics. 2019;11(7).

114. Sjöholm E, Mathiyalagan R, Rajan Prakash D, Lindfors L, Wang Q, Wang X, et al. 3D-Printed Veterinary Dosage Forms—A Comparative Study of Three Semi-Solid Extrusion 3D Printers. Pharmaceutics. 2020;12(12).

115. Johannesson J, Khan J, Hubert M, Teleki A, Bergström CAS. 3D-printing of solid lipid tablets from emulsion gels. International Journal of Pharmaceutics. 2021;597:120304.

116. Liu J, Tagami T, Ozeki T. Fabrication of 3D-Printed Fish-Gelatin-Based Polymer Hydrogel Patches for Local Delivery of PEGylated Liposomal Doxorubicin. Marine drugs. 2020;18(6):325.

117. Naseri E, Cartmell C, Saab M, Kerr RG, Ahmadi A. Development of 3D Printed Drug-Eluting Scaffolds for Preventing Piercing Infection. Pharmaceutics. 2020;12(9):901.

118. Andriotis EG, Eleftheriadis GK, Karavasili C, Fatouros DG. Development of Bio-Active Patches Based on Pectin for the Treatment of Ulcers and Wounds Using 3D-Bioprinting Technology. Pharmaceutics. 2020;12(1):56.

119. Pereira BC, Isreb A, Forbes RT, Dores F, Habashy R, Petit J-B, et al. 'Temporary Plasticiser': A novel solution to fabricate 3D printed patient-centred cardiovascular 'Polypill' architectures. European Journal of Pharmaceutics and Biopharmaceutics. 2019;135:94-103.

120. Lopes CM, Bettencourt C, Rossi A, Buttini F, Barata P. Overview on gastroretentive drug delivery systems for improving drug bioavailability. Int J Pharm. 2016;510(1):144-58.

121. Liu H, Zhao W, Hu Q, Zhao L, Wei Y, Pi C, et al. Gastric floating sustained-release tablet for dihydromyricetin: Development, characterization, and pharmacokinetics study. Saudi Pharmaceutical Journal. 2019;27(7):1000-8.

122. Vithani K, Goyanes A, Jannin V, Basit AW, Gaisford S, Boyd BJ. An Overview of 3D Printing Technologies for Soft Materials and Potential Opportunities for Lipid-based Drug Delivery Systems. Pharmaceutical Research. 2018;36(1):4.

123. Liu F, Ranmal S, Batchelor HK, Orlu-Gul M, Ernest TB, Thomas IW, et al. Patient-centred pharmaceutical design to improve acceptability of medicines: similarities and differences in paediatric and geriatric populations. Drugs. 2014;74(16):1871-89.

124. Siepmann J, Faham A, Clas S-D, Boyd BJ, Jannin V, Bernkop-Schnürch A, et al. Lipids and polymers in pharmaceutical technology: Lifelong companions. International Journal of Pharmaceutics. 2019;558:128-42.

125. Rani S, Rana R, Saraogi GK, Kumar V, Gupta U. Self-Emulsifying Oral Lipid Drug Delivery Systems: Advances and Challenges. AAPS PharmSciTech. 2019;20(3):129.

126. Mandic J, Zvonar Pobirk A, Vrecer F, Gasperlin M. Overview of solidification techniques for self-emulsifying drug delivery systems from industrial perspective. Int J Pharm. 2017;533(2):335-45.

127. Pechenov S, Bhattacharjee H, Yin D, Mittal S, Subramony JA. Improving drug-like properties of insulin and GLP-1 via molecule design and formulation and improving diabetes management with device & drug delivery. Advanced Drug Delivery Reviews. 2017;112:106-22.

128. Murphy SV, Atala A. 3D bioprinting of tissues and organs. Nature biotechnology. 2014;32(8):773-85.

129. Groll J, Burdick JA, Cho DW, Derby B, Gelinsky M, Heilshorn SC, et al. A definition of bioinks and their distinction from biomaterial inks. Biofabrication. 2018;11(1):013001.

130. Jiang T, Munguia-Lopez JG, Flores-Torres S, Kort-Mascort J, Kinsella JM. Extrusion bioprinting of soft materials: An emerging technique for biological model fabrication. Applied Physics Reviews. 2019;6(1):011310.

131. Blaeser A, Duarte Campos DF, Puster U, Richtering W, Stevens MM, Fischer H. Controlling Shear Stress in 3D Bioprinting is a Key Factor to Balance Printing Resolution and Stem Cell Integrity. Adv Healthc Mater. 2016;5(3):326-33.

132. Kuang X, Chen K, Dunn CK, Wu J, Li VCF, Qi HJ. 3D Printing of Highly Stretchable, Shape-Memory, and Self-Healing Elastomer toward Novel 4D Printing. ACS Applied Materials & Interfaces. 2018;10(8):7381-8.

133. Gao B, Yang Q, Zhao X, Jin G, Ma Y, Xu F. 4D Bioprinting for Biomedical Applications. Trends Biotechnol. 2016;34(9):746-56.

134. Wan Z, Zhang P, Liu Y, Lv L, Zhou Y. Four-dimensional bioprinting: Current developments and applications in bone tissue engineering. Acta Biomaterialia. 2020;101:26-42.

135. Derakhshanfar S, Mbeleck R, Xu K, Zhang X, Zhong W, Xing M. 3D bioprinting for biomedical devices and tissue engineering: A review of recent trends and advances. Bioactive Materials. 2018;3(2):144-56.

136. Peng W, Datta P, Ayan B, Ozbolat V, Sosnoski D, Ozbolat IT. 3D bioprinting for drug discovery and development in pharmaceutics. Acta Biomater. 2017;57:26-46.

137. Noor N, Shapira A, Edri R, Gal I, Wertheim L, Dvir T. 3D Printing of Personalized Thick and Perfusable Cardiac Patches and Hearts. Advanced Science. 2019;6(11):1900344.

138. Isaacson A, Swioklo S, Connon CJ. 3D bioprinting of a corneal stroma equivalent. Exp Eye Res. 2018;173:188-93.

139. Pourchet LJ, Thepot A, Albouy M, Courtial EJ, Boher A, Blum LJ, et al. Human Skin 3D Bioprinting Using Scaffold-Free Approach. Adv Healthc Mater. 2017;6(4).

140. Nadgorny M, Ameli A. Functional Polymers and Nanocomposites for 3D Printing of Smart Structures and Devices. ACS Applied Materials & Interfaces. 2018;10(21):17489-507.

141. Kong YL, Gupta MK, Johnson BN, McAlpine MC. 3D printed bionic nanodevices. Nano Today. 2016;11(3):330-50.

142. Ahn BY, Duoss EB, Motala MJ, Guo X, Park S-I, Xiong Y, et al. Omnidirectional Printing of Flexible, Stretchable, and Spanning Silver Microelectrodes. Science. 2009;323(5921):1590.

143. Zhu Z, Guo S-Z, Hirdler T, Eide C, Fan X, Tolar J, et al. 3D Printed Functional and Biological Materials on Moving Freeform Surfaces. Advanced Materials. 2018;30(23):1707495.

144. Muth JT, Vogt DM, Truby RL, Mengüç Y, Kolesky DB, Wood RJ, et al. Embedded 3D Printing of Strain Sensors within Highly Stretchable Elastomers. Advanced Materials. 2014;26(36):6307-12.

145. Yuk H, Lu B, Lin S, Qu K, Xu J, Luo J, et al. 3D printing of conducting polymers. Nature Communications. 2020;11(1):1604.

146. Agarwala S, Lee JM, Ng WL, Layani M, Yeong WY, Magdassi S. A novel 3D bioprinted flexible and biocompatible hydrogel bioelectronic platform. Biosensors and Bioelectronics. 2018;102:365-71.

147. Aggas JR, Abasi S, Smith B, Zimmerman M, Deprest M, Guiseppi-Elie A. Microfabricated and 3-D Printed Soft Bioelectronic Constructs from PAn-PAAMPSA-Containing Hydrogels. Bioengineering (Basel). 2018;5(4).

148. Mannoor MS, Jiang Z, James T, Kong YL, Malatesta KA, Soboyejo WO, et al. 3D Printed Bionic Ears. Nano Lett. 2013;13(6):2634-9.

149. Kong YL, Tamargo IA, Kim H, Johnson BN, Gupta MK, Koh T-W, et al. 3D Printed Quantum Dot Light-Emitting Diodes. Nano Letters. 2014;14(12):7017-23.

150. Adams JJ, Duoss EB, Malkowski TF, Motala MJ, Ahn BY, Nuzzo RG, et al. Conformal Printing of Electrically Small Antennas on Three-Dimensional Surfaces. Advanced Materials. 2011;23(11):1335-40.

151. Yu Y, Nyein HYY, Gao W, Javey A. Flexible Electrochemical Bioelectronics: The Rise of In Situ Bioanalysis. Advanced Materials. 2020;32(15):1902083.

152. Sun J, Zhou W, Yan L, Huang D, Lin L-y. Extrusion-based food printing for digitalized food design and nutrition control. Journal of Food Engineering. 2018;220:1-11.

153. Karyappa R, Hashimoto M. Chocolate-based Ink Three-dimensional Printing (Ci3DP). Scientific Reports. 2019;9(1):14178.

154. Yang F, Zhang M, Prakash S, Liu Y. Physical properties of 3D printed baking dough as affected by different compositions. Innovative Food Science & Emerging Technologies. 2018;49:202-10.

155. Liu Z, Bhandari B, Zhang M. Incorporation of probiotics (Bifidobacterium animalis subsp. Lactis) into 3D printed mashed potatoes: Effects of variables on the viability. Food Research International. 2020;128:108795.

156. Yang F, Zhang M, Bhandari B, Liu Y. Investigation on lemon juice gel as food material for 3D printing and optimization of printing parameters. LWT. 2018;87:67-76.

157. Cotabarren IM, Cruces S, Palla CA. Extrusion 3D printing of nutraceutical oral dosage forms formulated with monoglycerides oleogels and phytosterols mixtures. Food Research International. 2019;126:108676.

158. Ahmed J, Mulla M, Joseph A, Ejaz M, Maniruzzaman M. Zinc oxide/clove essential oil incorporated type B gelatin nanocomposite formulations: A proof-of-concept study for 3D printing applications. Food Hydrocolloids. 2020;98:105256.

159. Attaran M. The rise of 3-D printing: The advantages of additive manufacturing over traditional manufacturing. Business Horizons. 2017;60(5):677-88.

160. Skylar-Scott MA, Mueller J, Visser CW, Lewis JA. Voxelated soft matter via multimaterial multinozzle 3D printing. Nature. 2019;575(7782):330-5.

161. RegenHU. 3DDiscovery [Available from: https://www.regenhu.com/3d-bioprinters.

162. Envisiontec. 3D-Bioplotter [Available from: https://envisiontec.com/3d-printers/3d-bioplotter/.

163. Regemat. BIO V1 [Available from: https://www.regemat3d.com/tecnologias.

164. Cellink. Bio X [Available from: https://www.cellink.com/product/cellink-bio-x/.

165. FabRx. M3DIMAKER [Available from: https://www.fabrx.co.uk/technologies/.

166. Administration UFaD. Technical Considerations for Additive Manufactured Medical Devices -Draft Guidance for Industry and Food and Drug Administration Staff. https://www.fda.gov/downloads/MedicalDevices/DeviceRegulationandGuidance/GuidanceDocuments/UCM499809.pdf2016.

167. Aprecia. Spritam 2015 [Available from: https://www.aprecia.com/zipdose-platform/zipdose-technology.php.

168. Khairuzzaman A. Regulatory Perspectives on 3D Printing in Pharmaceuticals. In: Basit A, Gaisford S, editors. 3D Printing of Pharmaceuticals. AAPS Advances in the Pharmaceutical Sciences Series: Springer, Cham; 2018.

169. Edinger M, Bar-Shalom D, Rantanen J, Genina N. Visualization and Non-Destructive Quantification of Inkjet-Printed Pharmaceuticals on Different Substrates Using Raman Spectroscopy and Raman Chemical Imaging. Pharm Res. 2017;34(5):1023-36.

170. Trenfield SJ, Tan HX, Goyanes A, Wilsdon D, Rowland M, Gaisford S, et al. Non-destructive dose verification of two drugs within 3D printed polyprintlets. Int J Pharm. 2020;577:119066.

171. Trenfield SJ, Xian Tan H, Awad A, Buanz A, Gaisford S, Basit AW, et al. Track-and-trace: Novel anti-counterfeit measures for 3D printed personalized drug products using smart material inks. Int J Pharm. 2019;567:118443.

172. Edinger M, Bar-Shalom D, Sandler N, Rantanen J, Genina N. QR encoded smart oral dosage forms by inkjet printing. Int J Pharm. 2018;536(1):138-45.

173. Elder DP, Kuentz M, Holm R. Pharmaceutical excipients - quality, regulatory and biopharmaceutical considerations. Eur J Pharm Sci. 2016;87:88-99.

174. Xu X, Robles-Martinez P, Madla CM, Joubert F, Goyanes A, Basit AW, et al. Stereolithography (SLA) 3D printing of an antihypertensive polyprintlet: Case study of an unexpected photopolymer-drug reaction. Addit Manuf. 2020;33:101071.

175. Trenfield SJ, Awad A, Madla CM, Hatton GB, Firth J, Goyanes A, et al. Shaping the future: recent advances of 3D printing in drug delivery and healthcare. Expert Opin Drug Deliv. 2019;16(10):1081-94.

176. Trenfield SJ, Awad A, Goyanes A, Gaisford S, Basit AW. 3D Printing Pharmaceuticals: Drug Development to Frontline Care. Trends Pharmacol Sci. 2018;39(5):440-51.

Table 1. Examples of dosage forms and medical devices produced by SSE 3DP

Formulation type	Formulation details/Properties	API	Excipients	Ref.
Polypill	An osmotic pump and sustained release compartments	Captopril (18.5%), nifedipine (10.7%) and glipizide (3.5%)	Cellulose acetate, D-mannitol, PEG 6000, MCC, sodium starch glycolate and HPMC	(98)
	Combination of five different drugs via two release mechanisms	Pravastatin (20%), atenolol (30%), ramipril (15%), aspirin (28.62%) and hydrochlorothiazide (5.86%)	Cellulose acetate, D-mannitol, PEG 6000, sodium starch glycolate and PVP	(75)
	Three different drugs with programmed release profiles	Metformin hydrochloride, glyburide and acarbose (ND%)	Pluronic F-127	(99)
	Controlled release fixed dose combination comprising of three anti-HIV-1 drugs	Efavirenz (25.5%), tenofovir disoproxil fumarate (12.8%) and emtricitabine (8.5%)	Brown humic acid sodium salt, hydroxyethylcellulose ethoxylate, quaternized and cellulose acetate phthalate	(100)
Immediate release tablets	Immediate release tablets	Levetiracetam (ND%)	Polyvinyl alcohol-polyethylene glycol graft copolymer (PVA-PEG) and Polyvinylpyrrolidonevinyl acetate copolymer (PVP-PVAc)	(43)
	Immediate release tablets	Levetiracetam (ND%)	Polyvinyl alcohol-polyethylene glycol graft copolymer (PVA-PEG), Kollicoat IR	(44)
	Subdivided printlets as an alternative to the splitting of conventional tablets	Spironolactone and hydrochlorothiazide (ND%)	Lactose, corn starch, MCC, HPMC, sucrose and dextrin	(101)
	Immediate release tablets	Carbamazepine (24%)	Hydroxypropyl-β-cyclodextrin, HPMC, PVP, sodium carboxymethylcellulose and croscarmellose sodium	(89)
	Immediate release tablets	Puerarin (ND%)	PEG 4000	(49)
	Printlets fabricated with two-component cross-linkable gels	Prednisolone and bovine serum albumin (ND%)	Four-armed polyethylene glycol (PEG_4) and ε-caprolactone monomer (CL)	(79)
	Immediate release tablets with high drug loadings	Paracetamol (80%)	Croscarmellose sodium and PVP	(102)
	Immediate release tablets with high drug loadings in different geometries	Levetiracetam (96%)	Croscarmellose sodium and hydroxypropyl cellulose (HPC)	(103)
	Immediate release tablets with	Levetiracetam	Carboxymethylcellulose	(104)

	different volumes	(93%)	sodium, croscarmellose sodium and PVP	
	Immediate-release formulations using thermosensitive gelatin pastes	Ibuprofen (10%)	Gelatin, glycerine, MCC, mannitol, lactose and HPMC	(105)
Controlled release tablets	Controlled release bilayer tablets	Guaifenesin (81%)	HPMC, sodium starch glycolate and MCC	(106)
	Tablets with different composition and dissolution profiles	Naftodipil (20%)	HPMC, mannitol, PEG 4000 and Kollidon CL-F	(66)
	Semi-solid tablets	Theophylline (5.36%, 7.14% or 8.93%)	HPMC 4KM and 4EM	(107)
	Tablets with pre-designed structures	Glipizide (1.7%, 2%, 2.3%)	HPMC, lactose, MCC and PVP	(108)
	Gastro-floating tablets	Dipyridamole (8.5%, 7.25% 6.5%)	HPMC, MCC, lactose and PVP	(109)
	Floating sustained-release systems	Ricobendazole (ND%)	Gelucire 50/13	(50)
	Printable formulations after several days of storage	Levetiracetam (23.4%)	PVA-PVP copolymer, HPMC and silicon dioxide	(95)
	Sustained-release formulations using thermosensitive gelatin pastes	Diclofenac (6.45%)	Gelatin, glycerine, MCC, mannitol, lactose and HPMC	(105)
Chewable printlets	Clinical study, printlets prepared in a hospital setting with various flavours, colours, doses, and sizes	Isoleucine (ND%)	Sucrose, pectin and maltodextrin	(59)
	Chocolate-based printlets in different shapes resembling cartoon characters	Paracetamol and ibuprofen (ND%)	Bitter chocolate and corn syrup	(110)
	Lego™-like chewable bricks	Paracetamol and ibuprofen (ND%)	Locust bean gum and glycerol	(111)
	Gummies	Lamotrigine (ND%)	HPMC and gelatin	(23)
	Gummies	Ranitidine hydrochloride (ND%)	Corn starch, carrageenan, xanthan gum, gelatine	(93)
Orodispersible films (ODFs)	ODFs fabricated in a one-step-process using disposable syringes	Warfarin (1.3%)	HPC and PVA	(112)
	To develop a platform to support the extemporaneous production of ODFs	Levocetirizine hydrochloride (ND%)	Glycerine, glycine and titanium dioxide	(24)
	Multi-layered ODFs fabricated with in-process drying	Benzydamine hydrochloride (ND%)	Hydroxyethylcelulose (HEC) of different viscosity grades	(96)
	ODFs	Paracetamol (37.5%, 25% and 12.5%)	Maltodextrins with a dextrose equivalent equal to 6 and 12	(52)
	ODFs	Olanzapine (5%)	PEO, Kollidon VA 64, poloxamer 407 and poloxamer 188	(53)

	ODFs prepared in a hospital setting, in comparison with the established compounded formulations	Warfarin (1.5%)	Lactose monohydrate, HPC and propylene glycol (PG)	(113)
	ODFs for veterinary use	Prednisolone (1%)	PEO, HPC, pure liver powder	(114)
Solid self-emulsifying formulations	Solid self-microemulsifying printlets in various geometries	Fenofibrate (7%) and cinnarizine (7%)	Gelucire 44/14, Gelucire 48/16 and Kolliphor	(71)
	Solid lipid tablets	Fenofibrate (ND%)	Maisine CC, Captex 355 EP/NF, Capmul MCM EP, Soybean oil, Kolliphor EL, Tween 85 and methyl cellulose	(115)
	Self-emulsifying suppositories prepared in different sizes without the aid of moulds	Tacrolimus (0.12%)	Gelucire 44/14, Gelucire 48/16 and coconut oil	(20)
	Self-emulsifying suppositories with a size adapted for administration to rats	Tacrolimus (0.9%)	Gelucire 44/14 and coconut oil	(22)
Medical devices	Devices cured with UV light	Prednisolone (0.5%, 1% and 1.5%)	Silopren UV LSR 2030	(77)
	Patches	5-fluorouracil (ND%)	Poly(lactic-co-glycolic acid) PLGA and polycaprolactone (PCL)	(97)
	Hydrogel patches	Doxorubicin (ND%)	Semi-synthesized fish gelatin methacryloyl (F-GelMA), carboxymethyl cellulose sodium (CMC)	(116)
	Microneedles	Insulin (ND%)	Alginate, hydroxyapatite, calcium chloride	(78)
	Biopieces	Mupirocin (20%, 30% and 40%)	PLGA	(117)
	Patches	Propolis (56%)	Pectin from apple and β-cyclodextrin	(118)

*ND% (not clearly disclosed %)

Table